

The VLT-FLAMES Survey of Massive Stars: Observations centered on the Magellanic Cloud clusters NGC 330, NGC 346, NGC 2004, and the N11 region * **

C. J. Evans¹, D. J. Lennon², S. J. Smartt³, and C. Trundle³

¹ UK Astronomy Technology Centre, Royal Observatory Edinburgh, Blackford Hill, Edinburgh, EH9 3HJ, UK

² The Isaac Newton Group of Telescopes, Apartado de Correos 321, E-38700, Santa Cruz de La Palma, Canary Islands, Spain

³ Department of Physics & Astronomy, Queen's University Belfast, Belfast BT7 1NN, Northern Ireland, UK

Abstract. We present new observations of 470 stars using the Fibre Large Array Multi-Element Spectrograph (FLAMES) instrument in fields centered on the clusters NGC 330 and NGC 346 in the Small Magellanic Cloud (SMC), and NGC 2004 and the N11 region in the Large Magellanic Cloud (LMC). A further 14 stars were observed in the N11 and NGC 330 fields using the Ultraviolet and Visual Echelle Spectrograph (UVES) for a separate programme. Spectral classifications and stellar radial velocities are given for each target, with careful attention to checks for binarity. In particular, we have investigated previously unexplored regions around the central LH9/LH10 complex of N11, finding ~ 25 new O-type stars from our spectroscopy. We have observed a relatively large number of Be-type stars that display permitted Fe II emission lines. These are primarily not in the cluster cores and appear to be associated with classical Be-type stars, rather than pre main-sequence objects. The presence of the Fe II emission, as compared to the equivalent width of H α , is not obviously dependent on metallicity. We have also explored the relative fraction of Be- to normal B-type stars in the field-regions near to NGC 330 and NGC 2004, finding no strong evidence of a trend with metallicity when compared to Galactic results. A consequence of service observations is that we have reasonable time-sampling in three of our FLAMES fields. We find lower limits to the binary fraction of O- and early B-type stars of 23 to 36%. One of our targets (NGC 346-013) is especially interesting with a massive, apparently hotter, less luminous secondary component.

Key words. stars: early-type – stars: fundamental parameters – stars: emission-line, Be – binaries: spectroscopic – galaxies: Magellanic Clouds

1. Introduction

As part of a European Southern Observatory (ESO) Large Programme we have completed a new spectroscopic survey of massive stars in fields centered on open clusters in the Large and Small Magellanic Clouds (LMC and SMC respectively) and the Galaxy. The survey has employed the Fibre Large Array Multi-Element Spectrograph (FLAMES) instrument at the Very Large Telescope (VLT), that provides high-resolution ($R \sim 20,000$) multi-object spectroscopy over a 25' diameter field-of-view. The scientific motivations for the survey, and the observational information for the three Galactic clusters (NGC 3293, NGC 4755, and NGC 6611), were presented by Evans et al. (2005, hereafter Paper I).

In this paper we present the FLAMES observations in the Magellanic Clouds. The material presented is largely a discussion of the spectral classifications and radial velocities of each star, and provides a consistent and thorough overview of what is

a particularly large dataset. In parallel to this catalogue, subsets of the sample are now being analysed by different groups. The sources of photometry and astrometry used for target selection are given in Section 2, followed by details of the observations in Section 3, and then a discussion of the observed sample.

Two FLAMES pointings were observed in each of the Clouds, centered on NGC 346 and NGC 330 in the SMC, and on NGC 2004 and the N11 region (Henize 1956) in the LMC. NGC 346 is a young cluster with an age in the range of 1 to 3×10^6 yrs (Kudritzki et al. 1989; Walborn et al. 2000; Bouret et al. 2003; Massey et al. 2005), that has clearly undergone prodigious star formation. It is also the largest H II region in the SMC. The best source of spectroscopic information in NGC 346 is the study by Massey et al. (1989, hereafter MPG), who found as many O-type stars in the cluster as were known in the rest of the SMC at that time. High-resolution optical spectra of five of the O-type stars from MPG were presented by Walborn et al. (2000, together with AzV 220 that is also within the FLAMES field-of-view). These were analysed by Bouret et al. (2003), in conjunction with ultraviolet data, to derive physical parameters.

N11 is also a relatively young region and includes the OB associations LH9, LH10 and LH13 (Lucke & Hodge 1970),

that are of interest in the context of sequential star-formation, see Walborn & Parker (1992), Parker et al. (1992, hereafter P92), and Barbá et al. (2003). P92 illustrated how rich the region is in terms of massive stars, presenting observations of 43 O-type stars in LH9 and LH10, with three O3-type stars found in LH10. These O3 stars were considered by Walborn et al. (2002) in their extension of the MK classification scheme to include the new O2 subtype, with one of the stars from P92 reclassified as O2-type. The FLAMES observations in N11 presented an opportunity to obtain good-quality spectroscopy of a large number of known O-type stars, whilst also exploring the spectral content of this highly-structured and dynamic region.

NGC 330 and NGC 2004 are older, more centrally condensed clusters. NGC 330 in particular has been the focus of much attention in recent years. Feast (1972) presented H α spectroscopy of 18 stars in the cluster, and noted: ‘It is also an object of considerable importance in discussion of possible differences between stars of the same age in the SMC and in the Galaxy’. The community has clearly taken his words to heart – in the past 15 years there have been numerous studies in the cluster, most of which were concerned with the large population of Be-type stars therein, namely Grebel et al. (1992), Lennon et al. (1993), Grebel et al. (1996), Mazzali et al. (1996), Keller & Bessell (1998), Keller et al. (1999), Maeder et al. (1999), and Lennon et al. (2003). The paper from these with the widest implications is that from Maeder et al. (1999), who compared the fraction of Be stars (relative to all B-type stars) in a total of 21 clusters in the SMC, LMC and the Galaxy. The fraction of Be stars appears to increase with decreasing metallicity, although their study was limited to only one cluster (NGC 330) in the SMC. This trend led Maeder et al. to advance the possibility of faster rotation rates at lower metallicities – one of the key scientific motivations that prompted this FLAMES survey.

In contrast to NGC 330, with the exception of abundance analyses of a few B-type stars by Korn et al. (2002, 2005), relatively little was known about the spectroscopic content of NGC 2004 until recently. A new survey by Martayan et al. (2006), also with FLAMES, has observed part of the field population near NGC 2004 using the lower-resolution mode of the Giraffe spectrograph (and with a different field-centre to ours). Martayan et al. concluded that the Be-fraction in their LMC field is not significantly different to that seen in the Galaxy.

The FLAMES observations for the current survey were obtained in service mode and so span a wide range of observational epochs, giving reasonable time-sampling for the detection of binaries. There are surprisingly few multi-epoch, multi-object spectroscopic studies of stellar clusters in the literature in this respect, with one such study in 30 Doradus summarized by Bertrand et al. (1998). Placing a lower limit on the binary fraction in dense star-forming regions such as NGC 346 and N11, combined with stellar rotation rates, will help to provide useful constraints in the context of star formation and the initial mass function.

2. Target selection

2.1. SMC photometry

The adopted photometry and astrometry for the targets in NGC 346 and NGC 330 is that from the initial ESO Imaging Survey (EIS) pre-FLAMES release by Momany et al. (2001).

2.2. N11 photometry

The N11 region was not covered by the EIS pre-FLAMES Survey and so we obtained 60s B and V images with the Wide Field Imager (WFI) at the 2.2-m Max Planck Gesellschaft (MPG)/ESO telescope, on 2003 April 04. These were processed by Dr. M. Irwin using a modified version of the Isaac Newton Telescope–Wide Field Camera (INT–WFC) data reduction pipeline (Irwin & Lewis 2001), we then calibrated the photometry to the Johnson-Cousins system using results from P92.

As in Paper I, for photometric calibration we prefer to visually match stars using published finding charts. In crowded regions such as those in our FLAMES fields this ensures accurate cross-identification. Cross-referencing the finding charts of P92 with the WFI images yielded matches of 41 stars (for which both B and V WFI photometry were available), with relatively sparse sampling in terms of $(B - V)$. To increase the number of cross-matched stars an astrometric search was performed between the WFI sources and the full P92 catalogue (available on-line at the Centre de Données astronomiques de Strasbourg). The mean (absolute) offsets found between the WFI and P92 astrometry (for the 41 stars with visual matches), were $\langle |\Delta\delta| \rangle \sim 0.4''$ and $\langle |\Delta\alpha| \rangle \sim 0.06''$; these were used to then expand the sample to 60 stars, with $V < 17.0$. The V and B colour terms found for the WFI data in N11 are shown in Figures 1 and 2, and the transformation equations found were:

$$V_J = V_{\text{WFI}} - 0.07 \times (B - V)_J - 0.34, \quad (1)$$

$$B_J = B_{\text{WFI}} + 0.26 \times (B - V)_J - 0.12. \quad (2)$$

After transformation we find mean (absolute) differences of $\sim 0.05^m$, with $\sigma \sim 0.05^m$ for both V and $(B - V)$. In the centre of LH 10, in which there is significant nebular emission, the INT–WFC pipeline detected some of the sources as ‘noise-like’ and did not yield sensible results; for these 11 stars (marked with a * in Table 6) the photometry here is that from P92. Their photometry is also included in the Table for N11-105 which was in the gap between CCDs in the WFI V -band image.

2.3. NGC 2004 photometry

NGC 2004 was observed in two of the EIS pre-FLAMES fields, LMC 33 and 34. At the time of the FLAMES observations a full EIS data release was not available for these fields, so the raw images were acquired from the ESO archive and reduced using the INT–WFC pipeline (also by Dr. M. Irwin).

CCD photometry in NGC 2004 has been published by Bencivenni et al. (1991) and Balona & Jerzykiewicz (1993). The former study is calibrated to the photographic work of

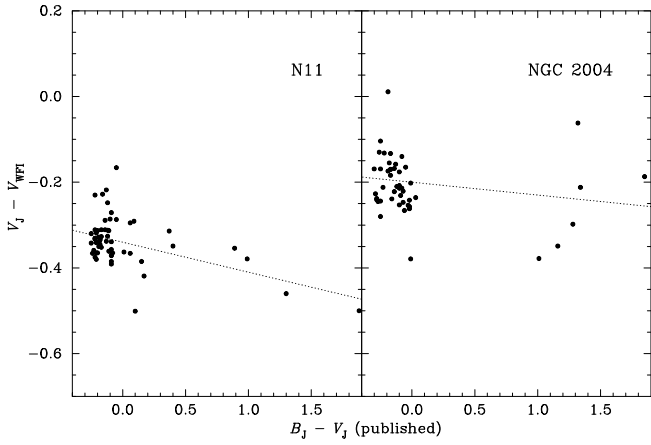


Fig. 1. Comparison of $V_J - V_{\text{WFI}}$ with published colours in N11 from Parker et al. (1992), and primarily from Robertson (1974) for NGC 2004.

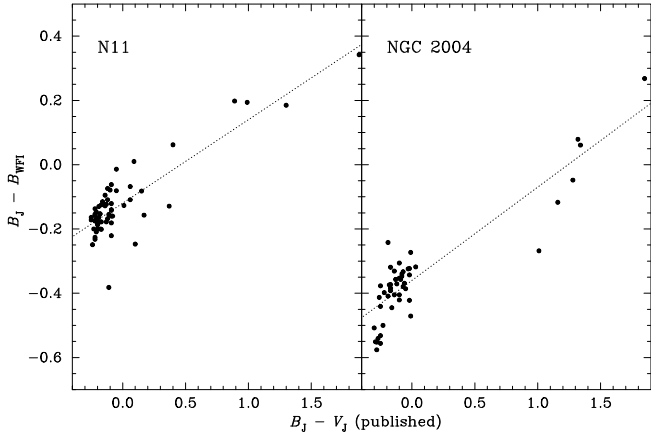


Fig. 2. Comparison of $B_J - B_{\text{WFI}}$ with published colours in N11 from Parker et al. (1992), and primarily from Robertson (1974) for NGC 2004.

Robertson (1974), albeit with consideration of two of the photoelectric standards from McGregor & Hyland (1984). The study by Balona & Jerzykiewicz is independent of previously published photometry in the cluster, however the ‘finding charts’ and format of the catalogue (in terms of pixel positions) are less than ideal for successfully recovering matched stars; without access to the raw frames, accurate cross-matching between their photometry and our WFI images cannot be ensured. Instead we employ visual matches of 48 stars from the identification charts of Robertson (1974) to calibrate the WFI data, taking photoelectric results from McGregor & Hyland (1984, 2 stars) and Walker (1987, 7 stars), with the data for the remaining 39 stars taken from Robertson. The V and B colour terms found for the NGC 2004 WFI data are also shown in Figures 1 and 2, and the transformation equations found were:

$$V_J = V_{\text{WFI}} - 0.03 \times (B - V)_J - 0.20, \quad (3)$$

$$B_J = B_{\text{WFI}} + 0.29 \times (B - V)_J - 0.36. \quad (4)$$

Whilst there is a relatively large scatter in $(V_J - V_{\text{WFI}})$, the colour term is very robust; the same result is found if only the photoelectric values are used or, similarly, if only the photographic results are used. After transformation we find mean (absolute) differences of $\sim 0.06^m$, with $\sigma \sim 0.04^m$ for both V and $(B - V)$.

2.4. Selection effects

Following similar methods to those in Paper I for target selection, the photometric data were used to create input catalogues for the FLAMES Fibre Positioner Observation Support Software (FPOSS) that allocates the Medusa fibres in a given field.

In Paper I we were perhaps too hasty with our description of avoiding known Be-type stars. To recap, the observed samples in the three Galactic clusters from Paper I were relatively complete for blue stars in the FLAMES pointing, down to $\sim V=13$. In terms of the final samples no external selection effects were present with regard to Be-type stars, with only 12 stars classified as Be and one as Ae-type, from a combined total of 319 FLAMES and FEROS targets. It is worth noting that NGC 3293 and NGC 4755 are two of the three clusters included by Maeder et al. (1999) in their ‘inner Galaxy’ sample (with the lowest Be-fraction compared to normal B-type stars), i.e. both NGC 3293 and NGC 4755 have genuinely small numbers of Be-type stars.

As mentioned in Paper I, one of our primary objectives concerns the process of nitrogen enrichment in OB-type stars and its correlation (or not) with rotational velocities. Spectroscopic analysis of Be stars is more involved (i.e. difficult!) than for ‘normal’ B-type stars. Thus in our FPOSS input catalogue, in an attempt to ensure that we didn’t observe a preponderance of Be stars in NGC 330, we excluded 15 stars classified as Be-type from previous spectroscopy (Lennon et al. 1993; Keller & Bessell 1998). However, this isn’t such a strong selection effect as it may sound - all of the excluded stars are from the Robertson (1974) survey and therefore are in (or near to) the main body of the cluster. Obviously the FLAMES survey cannot be used to comment on the incidence of the Be-phenomenon in the cluster itself, but it could in principle offer constraints on the field population around the cluster. With regard to the non-cluster population, we also excluded 15 stars from Evans et al. (2004) that have emission in their Balmer lines. However, these are not necessarily Be-type stars as the narrow emission in many of the stars from Evans et al. is likely attributable to nebular origins (see discussion in their Section 7). Given the high density of potential targets in the field, the exclusion of the stars from Evans et al. is very unlikely to bias the final sample.

In NGC 2004, Keller et al. (1999) reported 42 Be-type stars from their photometric study. However, due to the relative dearth of published spectroscopy in this field at the time of our observations, no potential targets were excluded when using FPOSS for fibre configuration. Lastly, the only weighting in NGC 346 and N11 was to give higher priority of fibre-assignment to known OB-type stars from MPG and P92.

In summary, the only strong external bias in our observed targets was in the main body of NGC 330. A much stronger selection effect in both NGC 330 and NGC 2004 is that the sheer density of the cluster cores prevents Medusa fibres being placed so close together, with many stellar targets blended – in any one FLAMES pointing only a few stars near the centre could be observed with the Medusa fibres. Follow-up of these two clusters with integral field spectroscopy, such as that offered by FLAMES-ARGUS at the centre of the FLAMES field plate, is an obvious project to allow a comprehensive exploration of the cluster populations. However, the field populations of both NGC 330 and NGC 2004 should be a relatively unbiased sample of the true population, subject to cluster membership issues and the faint magnitude cut-off of the FLAMES survey. These issues are discussed further in Section 8.4.

3. Observations and data reduction

3.1. FLAMES-Giraffe spectroscopy

All of the FLAMES observations were obtained in service mode, with the majority acquired over a 6 month period from 2003 July to 2004 January. The same high-resolution settings were used as for the Galactic observations, i.e. HR02 (with a central wavelength of $\lambda 3958 \text{ \AA}$), HR03 ($\lambda 4124$), HR04 ($\lambda 4297$), HR05 ($\lambda 4471$), HR06 ($\lambda 4656$), and HR14 ($\lambda 6515$). The bulk of the observations in NGC 330 were obtained prior to installation of a new grating in 2003 October, so the spectral coverage and resolution of these data are identical to that of our Galactic observations (see Paper I). However, the observations in NGC 346, NGC 2004 and N11 were taken with the new grating in place. The characteristics of the NGC 346 observations are given in Table 1. In comparison to the older grating the effective resolving power is decreased in some setups (in particular in the HR14 setting, yielding a correspondingly wider wavelength coverage), however the new grating is more efficient in terms of throughput.

In addition to observations at 6 central wavelengths, each field was observed at each wavelength for 6 exposures of 2275s. The repeat observations at each central wavelength were taken in batches of 3 exposures, each triplet forming an observing block for the ESO service programme. The observational constraints on our programme were not particularly demanding (the required seeing was 1.2" or better), but in some cases these conditions were not fully satisfied. Therefore, at some settings we have more than 6 observations, for instance the HR14 setting was observed 9 times in our NGC 346 field. Although the conditions may not have been ideal for every observing block, *all* the completed observations were reduced – in general the seeing was not greater than 1.5" and the data are of reasonable quality. This is of particular relevance in terms of the radial velocity information contained in the spectra. The majority of the observations in NGC 330 were spread over a relatively short time (~ 10 days). Otherwise we have reasonable time coverage, e.g. the NGC 346 observations spanned almost 3 months so we are in an excellent position to detect both single and double-lined binaries. In Appendix A we list the modified Julian dates (MJD) of each of the observations.

The data were reduced using the Giraffe Base-Line Reduction Software (girBLDRS), full details of which are given by Blecha et al. (2003). For consistency with our performance tests in Paper I, v1.10 of girBLDRS was used. More recent releases include the option to perform sky subtraction within the pipeline, but we prefer to employ the methods discussed in Paper I.

The final signal-to-noise is, of course, slightly variable between the different wavelength regions for a given target depending on the exact conditions when the observations were taken. As a guide, the signal-to-noise of the reduced, co-added spectra is ~ 200 for the brightest stars in each field, decreasing to 110 in N11 (with the brightest faint cut-off), 75 in NGC 2004, and 60 in NGC 346. Inspection of the reduced spectra in the NGC 330 field revealed particularly low signal-to-noise in the six HR03 observations. The Si II and Si IV lines that are important for quantitative analysis are included in this region, so the NGC 330 field was reobserved with the HR03 setup on 2005 July 20 & 24. These more recent observations are included in Table A.2 as HR03#07-12. The spectra were reduced using the same routines and software as the rest of the survey.

The NGC 330 field features the faintest stars in the entire survey. Besides the problems with the initial HR03 observations, the signal-to-noise ratio of the fainter stars in this field (even in the co-added spectra) decreases to ~ 35 -40 per unbinned pixel (at $V = 16$) and down to 25-30 for the very faintest stars. Binning of the data helps to some degree, but it is clear that detailed analysis of individual stars (such as those presented by Hunter et al., submitted) will not be feasible for some of the faintest targets. Nevertheless, the data presented here serve as a novel investigation of the spectral content of the region.

3.2. FLAMES-UVES spectroscopy

In addition to observations with the Giraffe Spectrograph, one can observe up to an additional 6 objects simultaneously with the red-arm of UVES (with a central wavelength setting of 5200 \AA). In the SMC and LMC fields the UVES fibres were used to observe a small number of 'red' targets. The FLAMES-UVES $\lambda 5200$ set-up gives spectral coverage from approximately $\lambda 4200$ to 5150 and 5250 to 6200 \AA (with the break in coverage arising from the gap between the two CCDs). These data were reduced by Dr. A. Kaufer using the standard pipeline (Ballester et al. 2004), which runs under MIDAS and performs the extraction, wavelength calibration, background subtraction and subsequently merges the individual orders to form two continuous spectra, i.e., from $\lambda 4200$ to $\lambda 5150$ and $\lambda 5250$ to $\lambda 6200 \text{ \AA}$.

Note that these data were observed over multiple epochs, and the pipeline does not correct the spectra to the heliocentric frame. For the purposes of approximate classification the very large number of individual UVES spectra were simply co-added, without correction to the heliocentric frame. Therefore we do not quote radial velocities for these stars.

Table 1. Summary of the wavelength coverage, mean FWHM of the arc lines and effective resolving power, R , at each Giraffe central wavelength setting, λ_c , for the observations in NGC 346.

Setting	λ_c (Å)	Wavelength coverage (Å)	FWHM		R
			(Å)	(pixels)	
HR02	3958	3854-4051	0.18	3.7	22,000
HR03	4124	4032-4203	0.15	3.4	27,500
HR04	4297	4187-4394	0.19	3.5	22,600
HR05	4471	4340-4587	0.23	3.7	19,450
HR06	4656	4537-4760	0.20	3.5	23,300
HR14	6515	6308-6701	0.39	3.9	16,700

3.3. Additional UVES spectroscopy in N11 and NGC 330

Normal UVES spectroscopy of a further 14 stars was obtained in 2001 November 1-3, as part of programme 68.D-0369(A); these data are included here to supplement the FLAMES sample. The spectra cover $\lambda 3750$ to $\lambda 5000$, $\lambda 5900$ to $\lambda 7700$, and $\lambda 7750$ to $\lambda 9600$ Å, at a resolving power of $R \sim 20,000$. These data were also reduced using the UVES pipeline, contemporaneously to those presented by Trundle et al. (2004).

The 9 targets in N11 complement the FLAMES programme well, providing a number of sharp-lined, luminous early B-type spectra. The spectra of the 5 targets in NGC 330 were only examined after collation of the FLAMES data hence their inclusion (out of sequence) at the end of Table 5. Note that the 14 stars observed with UVES in the traditional (non-fibre) mode are marked in Tables 5 and 6 as simply ‘UVES target’ (cf. ‘FLAMES-UVES target’ for those observed in the more limited, fibre-fed mode).

4. Spectral classifications and stellar radial velocities

The FLAMES spectra were classified by visual inspection, largely following the precepts detailed in Paper I, with additional consideration of the lower metallicity of stars in the LMC and SMC. The principal reference for O- and early B-type spectra is the digital atlas from Walborn & Fitzpatrick (1990), with the effects of metallicity explored by Walborn et al. (1995, 2000). Later-type stars in the SMC were classified using the criteria outlined by Lennon (1997), Evans & Howarth (2003), and Evans et al. (2004). In the LMC, A-type supergiants were classified from interpolation between the Galactic and SMC spectra given by Evans & Howarth, and B-type supergiants were classified with reference to Fitzpatrick (1988, 1991). Intermediate types of B0.2 and B0.7 have been used for some spectra – these are interpolated types that, in an effort to avoid metallicity effects, are largely guided by the intensity of the weak He II $\lambda 4686$ line.

Assignment of luminosity classes in early B-type stars, with due attention to metallicity effects and stellar rotation rates, can be difficult. Very subtle changes in the observed spectra can yield different classes. Indeed, the reason that we do not regularly employ the class IV notation for stars in the

Magellanic Clouds, arises from these issues – in a large dataset such as the FLAMES survey, one should be careful not to over-emphasize groupings as ‘dwarfs’ and ‘giants’, remembering that luminosity and gravity are continuous quantities. Also, as in our previous studies, we are cautious with regard to employing the Be notation – many of our targets have H α profiles displaying narrow core emission, accompanied by [N II] emission lines which are clearly nebular in origin. Where possible we give precise classifications for the Be spectra. In those spectra with Fe II emission (discussed further in Section 6) contamination of lines such as Si III $\lambda 4552$ makes classification more difficult. However, as for normal B-type stars, other absorption features are also of use as temperature diagnostics, such as O II $\lambda \lambda 4415-17$ and the O II/C III blend at $\lambda 4650$ Å (remembering to account for metallicity effects). Of course, our Be classifications do not consider the likely contribution to the continuum by the emission region, and thus may not correlate to the same temperatures as for normal B stars.

In Tables 4, 5, 6, and 7 we present the observational properties of each of the stars observed in the four FLAMES fields in the Magellanic Clouds. Spectral classifications and stellar radial velocities are given, together with cross-references to existing catalogues and comments regarding the appearance of the H α profiles and binarity. For NGC 346, NGC 330 and NGC 2004 we also include the radial distance (r_d , in arcmin) of each star from the centre of the cluster core.¹

Finding charts are included for each of the fields in Figures 13, 14, 15, and 16. The finding charts employ images from the Digitized Sky Survey (DSS) with our targets overlaid. The WFI pre-imaging used for target selection is significantly superior to the DSS images, however our intent here is solely to give a clear overview of the locations of each of the stars in our sample. The DSS images provide such clarity, in particular they are free of the chip-gaps arising from the WFI CCD array. One clear point evident from the finding charts is that NGC 330 and NGC 2004 are very compact clusters and that, whilst the FLAMES observations sample some peripheral cluster members, the majority of the targets sample the local field population. Furthermore, the radius of the ionized region in NGC 346

¹ For completeness, the coordinates (J2000.0) used in calculating the radial distances were:

NGC 346: $\alpha = 00^{\text{h}}59^{\text{m}}18.0^{\text{s}}$, $\delta = -72^{\circ}10'48.0''$,

NGC 330: $\alpha = 00^{\text{h}}56^{\text{m}}18.8^{\text{s}}$, $\delta = -72^{\circ}27'47.2''$,

NGC 2004: $\alpha = 05^{\text{h}}30^{\text{m}}40.2^{\text{s}}$, $\delta = -67^{\circ}17'14.3''$.

is given by Relaño et al. (2002) as ~ 3.5 arcmin; many of the FLAMES targets are beyond this radius highlighting that, even in this pointing, the observations sample both the cluster and field population.

The N11 region is more complex, with both LH10 (the denser region above the centre in Figure 15) and LH9 (the relatively ‘open’ cluster just below centre). The *V*-band WFI image is shown in Figure 17, in false-colour to better highlight the nebulosity. The full complexity of the region is revealed in the original photographic plate from Henize (1956). Star N11-004 is the principal object in N11G, N11-063 and N11-099 are both in N11C, and some of our targets south of LH9 are in N11F. Further insight into the structure of this region is given by the $H\alpha + [N II]$ photograph from Malcolm G. Smith published by Walborn & Parker (1992), and from a near-IR image from Dr. R. Barbá (private communication), both of which show a wide variety of arcs and filaments of nebular gas.

Radial velocities (v_r in km s^{-1}) are given for each star, excepting those that appear to be multiple systems. The measurements here are the means of manual estimates of a number of line centres, as indicated in parentheses in the tables. The primary lines used are generally those of He I, He II and Si III, with a typical standard deviation of the individual measurements around $5\text{--}10 \text{ km s}^{-1}$. We prefer manual measurements such as these because of the highly variable nebular contamination in a region such as NGC 346 (which may lead to spurious results if more automated methods are employed). In a small number of stars with apparently large rotational velocities (or lower signal-to-noise), precise determination of the line centres is more difficult thereby yielding a less certain value, as indicated here using the usual ‘:’ identifier in the tabulated results. The precision of manual measurements may also be biased by the infilling of helium lines, either by nebular contamination in morphologically normal spectra, or by infilling of the lines in Be-type stars; where these effects are obvious we have avoided the relevant lines but naturally there may be cases in which the effects are not so prominent yet affect the (apparent) line centre.

In tables 4, 5, 6, and 7 we present stellar radial velocities for each of our targets. In the process of measuring the velocities we find a relatively large number of spectra displaying evidence of binarity. These are shown in the tables as ‘Binary’, with SB1 and SB2 added to indicate single-lined and double-lined binaries where it was possible to identify the nature of the system. Finally, in the comments column of each table we note a small number of stars as ‘variable v_r ?’. In these one or two lines have anomalous velocities, with it unclear whether they arise from binarity.

4.1. Cross-references with x-ray observations

We have cross-referenced our FLAMES targets in the N11 and NGC 346 fields with the x-ray sources from Nazé et al. (2003, 2004a,b). We find that NGC 346-067 is $\sim 1.9''$ from source #6 in the Nazé et al. (2003) study. In fact, it is the same counterpart suggested by them, i.e. MA93#1038 (Meyssonnier & Azzopardi 1993). The tabulated separation

between optical and x-ray positions is $0.5''$, suggesting a small offset between their astrometric solution and that from the EIS data. Widening our search radius from $3''$ to $5''$ we find one further potential cross-match: NGC 346-078 (an early B-type binary) is $3.8''$ from their source #17; although in the opposite sense to NGC 346-067 and #6 and it seems unlikely that this is a valid match.

Similar searches with the *XMM-Newton* sources reported by Nazé et al. (2004a) in N11, and additional sources in NGC 346 from Nazé et al. (2004b), revealed no further cross-matches with our FLAMES sample, suggesting that none of our observed stars (excepting NGC 346-067) are particularly strong x-ray sources.

5. Comments on individual stars

There is a tremendous amount of new spectroscopic information available in our LMC and SMC fields. In nearly all cases the FLAMES spectra offer significantly better-quality data than previously. Also of note is that many stars, particularly in the NGC 330 and NGC 2004 fields, have not been observed before spectroscopically.

In the following sections we discuss spectra with interesting or peculiar morphologies. In general we do not address the specific details of detected binaries, restricting ourselves to simply indicating their binarity in Tables 4, 5, 6, and 7. In many cases the FLAMES spectra are sufficient to determine orbital periods and, for some systems, offer an insight into the physical nature of the individual components. A comprehensive treatment of the binary spectra will be presented elsewhere. Emission-line (i.e. Oe and Be) stars are discussed separately in Section 6.

5.1. NGC 346-001

NGC 346-001 is the well-studied star Sk 80 (Sanduleak 1968), also identified as AzV 232 (Azzopardi & Vigneau 1975, 1982) and MPG 789. It was classified as O7 Iaf+ by Walborn (1977), with the f+ suffix employed to denote the strong Si IV $\lambda 4116$, N III $\lambda 4634\text{--}40\text{--}42$, and He II $\lambda 4686$ emission features; indeed, Sk 80 serves as the principal O7 supergiant in the Walborn & Fitzpatrick (1990) spectral atlas. A detailed atmospheric analysis of a VLT-UVES spectrum of this star was given by Crowther et al. (2002).

Close inspection of the individual FLAMES-Giraffe spectra reveals several features that suggest this object to be a binary. Perhaps the most distinctive of these is shown in Figure 3. In the first five exposures there is a weak absorption feature in the blueward wing of the He II $\lambda 4686$ emission line (left-hand panel of figure). Compare this to the HR06/#06, #07 and #08 frames in which it is absent, with slightly weaker $\lambda 4686$ emission (right-hand panel). From the same observations, a small shift ($\sim 10 \text{ km s}^{-1}$) is seen in the He I $\lambda 4713$ line. A similar, though less significant effect to that seen in the $\lambda 4686$ line, is also seen in the blueward wing of the $H\alpha$ profile (we do not consider the core intensity given the problems of nebular subtraction). Inspection of the spectra from the HR05 observations (which also include He II $\lambda 4542$) reveals a shift of ~ 10

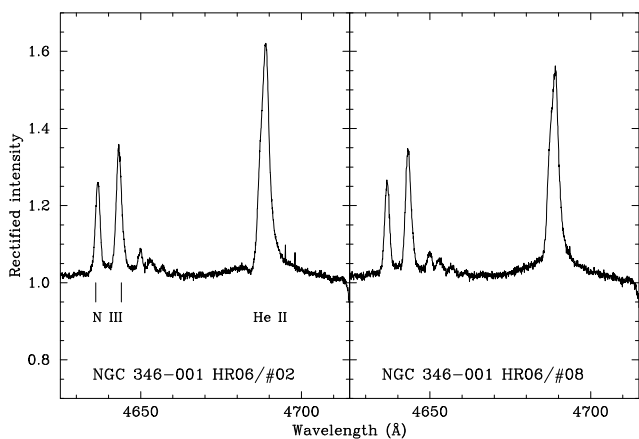


Fig. 3. Variations in the He II $\lambda 4686$ line seen in NGC 346-001. The left panel shows exposure HR06/#02, with the right panel showing HR06/#08, note that the intensity of the N III $\lambda 4634$, 4640 - 41 emission is identical whereas the He II $\lambda 4686$ morphology and intensity differs.

km s^{-1} between the two epochs, which is also mirrored in the He I $\lambda 4471$ line. That these shifts are seen in the mainly photospheric He I features suggests there is a companion and that we are not seeing evidence of wind variability.

Compared to the VLT-UVES data from Crowther et al., the resolving power from the high-resolution mode of FLAMES-Giraffe is roughly a factor of two lower, but the signal-to-noise of the new spectrum is ~ 400 . Aside from consideration of binarity, we note the presence of two weak emission lines that we attribute to N III, with rest wavelengths of $\lambda 3938.5$ and $\lambda 4379.0$ (Dr. F. Najarro, private communication). Upon reinspection of the UVES spectrum from Crowther et al. these features can also be seen, but are less obvious due to the inherent problems associated with blaze removal etc. The $\lambda 4379.0$ line can also be seen in the high-resolution spectrum presented by Walborn et al. (1995), although there are some comparable artifacts nearby; the line is also seen in emission in AzV 83 (Walborn et al. 2000).

5.2. NGC 346-007

High-resolution optical spectra of NGC 346-007 (MPG 324) have been published by Walborn et al. (1995, NGC346#6) and Walborn et al. (2000). In the FLAMES spectrum the Si IV $\lambda 4116$ feature is very weakly in emission (such that it was within the noise level of previous spectra) and therefore the Walborn et al. classification of O4 V((f)) is revised slightly to O4 V((f+)) to reflect this. Small radial velocity shifts are seen in some lines in the spectra of NGC 346-007 (of order 20 - 30 km s^{-1}) suggesting it as a single-lined binary.

5.3. NGC 346-013

This object is one of the most intriguing in the FLAMES survey. At first glance the spectrum is that of an early B-type star

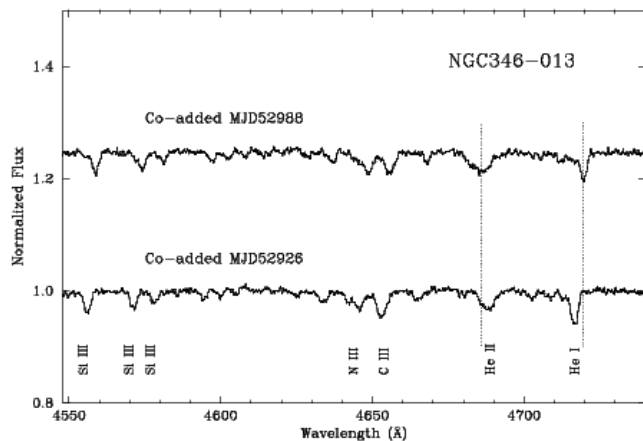


Fig. 4. The HR06 observations of NGC 346-013. The spectra from the two epochs have been co-added, and then 11-pixel median filtered to aid clarity. Identified lines are Si III $\lambda\lambda 4552$ - 68 - 75 ; N III $\lambda\lambda 4634$, 4640 - 42 ; C III $\lambda 4650$; He II $\lambda 4686$; He I $\lambda 4713$. The vertical dotted lines highlight the wavelengths of the He I and II lines in the second batch of observations; these are seen to move in an opposite sense between epochs.

with a spectral type of B1 or B1.5, but there is also anomalous absorption from He II $\lambda 4686$. Inspection of the individual spectra reveals significant velocity shifts in the He I and Si III absorption lines, with a maximum amplitude over the time coverage of the FLAMES observations of approximately 400 km s^{-1} . Other lines such as the C III and N III blends move in the same sense. Interestingly, the He II $\lambda 4686$ moves in the *opposite* sense to the other features and with a smaller amplitude, suggesting that it is the more massive object in the system (and presumably hotter by virtue of the 4686 line). These features are illustrated in Figure 4.

We lack other diagnostics of the companion associated with the He II $\lambda 4686$ feature in the current data. The He I $\lambda 4471$ absorption appears to be marginally double-lined in the first three HR05 observations, but it is within the noise level preventing accurate characterization. No strong absorption is seen from He II $\lambda 4542$ in the HR04 data suggesting a narrow temperature range for the companion. We note that NGC 346-013 does not appear in the x-ray catalogue of Nazé et al. (2003). A more detailed treatment of its orbital properties will be presented elsewhere. Further spectroscopic monitoring of this object is clearly a high priority.

5.4. NGC 346-026, & NGC 346-028

High-resolution echelle spectra of NGC 346-026 (MPG 012) and NGC 346-028 (MPG 113) were presented by Walborn et al. (2000), with a detailed discussion of their morphologies. For NGC 346-028 we adopt the Walborn et al. classification of OC6 Vz. In the case of NGC 346-026 we prefer the unique classification of B0 (N str), over the O9.5-B0 (N str) from Walborn et al. The line that is least consistent with a B0-type is He II $\lambda 4200$, which is marginally

stronger in NGC 346-026 than in ν Ori, the B0 V standard (Walborn & Fitzpatrick 1990) – given the ‘N str’ remark, perhaps part of the explanation for this lies with a stronger $\lambda 4200$ N III line. Interestingly, the Si IV lines in the spectrum are in reasonable agreement with those in ν Ori, which is surprising given the lower metallicity of the SMC. This point strengthens the suggestion by Walborn et al. that luminosity class IV might be more befitting of the star, *a priori* of the luminosity and gravity results found by Bouret et al. (2003). Thus, we classify the star as B0 IV (N str).

5.5. N11-020

The spectrum of N11-020 displays broad, asymmetric H α emission, combined with strong N III $\lambda 4634$ -41 and He II $\lambda 4686$ emission. Such morphology is similar to that seen in ζ Pup (Walborn & Fitzpatrick 1990). The FLAMES spectrum appears slightly cooler than ζ Pup, resulting in the classification of O5 I(n)fp. There are clear variations in both the H α and He II $\lambda 4686$ lines, which could be indicative of wind variability. However, close inspection of other lines such as He II $\lambda 4542$ and H δ reveal subtle morphological changes indicative of a companion, suggesting that N11-020 is a further binary.

5.6. N11-026, N11-014 & N11-091

The spectrum of N11-026 is shown in Figure 5 and is between the O2 and O3-type standards published by Walborn et al. (2002, 2004). Thus we employ an intermediate type of O2.5 III(f*). N11-026 is $\sim 4.5'$ to the north of LH10 (see Figure 15) and the photograph of N11 from Walborn & Parker (1992) shows a likely ionization front just to the east of the star. In fact, the FLAMES targets adjacent to #026 offer a good illustration of the rich star-formation history of the region. Cross-matching our targets again with the image from Walborn & Parker (1992), N11-014 (to the west of #026) is a B2 supergiant in a more rarefied region, and N11-091 is an O9-type spectroscopic binary (with what appears to be a B-type secondary) lying in a dense knot of gas.

N11-026 has the third largest velocity in the N11 targets, with $v_r = 330 \text{ km s}^{-1}$ (with standard deviation, $\sigma = 5$). The median result for the N11 stars with measured radial velocities is 295 km s^{-1} suggesting N11-026 as a run-away object, cf. the usual criterion of $\Delta v_r \sim 40 \text{ km s}^{-1}$ (Blaauw 1961). N11-026 is $\sim 1'$ away from N11-091, which at the distance of the LMC corresponds to $\sim 14 \text{ pc}$. An ejected young star could conceivably cover this distance in its short lifetime (such arguments are discussed in their definition of a field star by Massey et al. 1995). Indeed, in 2 Myr the star may have even travelled the $\sim 70 \text{ pc}$ from the northern edge of LH10.

5.7. N11-028

N11-028 is the primary star of N11A, a well-studied nebular knot to the north-east of LH10 (N11B). Heydari-Malayeri & Testor (1985) suggested that the principal source of ionization was a star with $T_{\text{eff}} \sim 44,000 \text{ K}$, i.e. an

O-type star. This was confirmed by P92, who found an embedded primary (their star 3264) with two faint companions. P92 show the spectrum of 3264 in their Figure 5, classifying it as O3-6 V. The uncertainty in the classification arises from the strong nebular emission in the spectrum, as one would expect from the near-IR study by Israel & Koornneef (1991) who concluded that N11A was dominated by such emission.

More recently, impressive images of N11A from the Wide Field Planetary Camera 2 (WFPC2) on the *Hubble Space Telescope* were published by Heydari-Malayeri et al. (2001). Their imaging (see their Figure 2) revealed at least five objects in the core of N11A, which they labelled as numbers 5 to 9. Their star #7 was the brightest with Strömgren $v = 14.59$, with three of the others (5, 6, and 9) fainter than 18th magnitude.

In the WFI imaging used to select our FLAMES targets, N11A appears as an unresolved, dense blob, with the fibre placed on the bright core. Our photometric methods here are relatively simple and were primarily concerned with target selection. The multiplicity in N11A, combined with the effects of the nebulosity, highlight that a more tailored photometric analysis is warranted for a star such as this, beyond the scope of our programme (and imaging). As such, the quoted magnitude in Table 6 is brighter than that given by P92 and Heydari-Malayeri et al. (2001).

The MEDUSA fibres used with FLAMES have an on-sky aperture of $1.2''$. From comparisons with the figure from Heydari-Malayeri et al., it is likely that the MEDUSA fibre was not centered perfectly on the principal star (owing to the resolution of the WFI image). It is also possible that the FLAMES spectrum may include some contribution from their star #8, which is two magnitudes fainter than the primary.

The FLAMES spectrum of N11-028/Parker 3264 is shown in Figure 6, and is classified here as O6-8 V, cf. O3-6 V from P92. We see no obvious evidence of binarity, or of other features from a possible companion. The absorption at He I $\lambda 4026$ is larger than that seen in He II $\lambda 4200$, thereby requiring a spectral type of O6 or later. The uncertainty in the current classification arises because of the He I $\lambda 4471$ line, in which the degree of infilling is unclear. Obviously such a revision of spectral type will have a significant effect on the perceived ionizing flux in the nebula. Indeed, Heydari-Malayeri et al. (2001) concluded that an O7.5 or O8 main-sequence star could account for the observed ionization, commensurate with our classification. One interesting feature is the weak Mg II $\lambda 4481$ absorption sometimes seen in mid O-type spectra (e.g. Morrell et al. 1991), attributed by Mihalas (1972) to deviations from the assumptions of local thermodynamic equilibrium, i.e. non-LTE effects.

5.8. N11-038

There is a striking similarity between the spectrum of this star and that of AzV 75 in the SMC (Walborn et al. 2000), with the spectrum here classified as O5 III(f+). Interestingly this star was observed by P92 (their star 3100) and classified as ‘O6.5 V((f))’. The FLAMES data shows strong He II absorption at $\lambda 4200$, cf. the P92 spectrum in which it is relatively weak. The

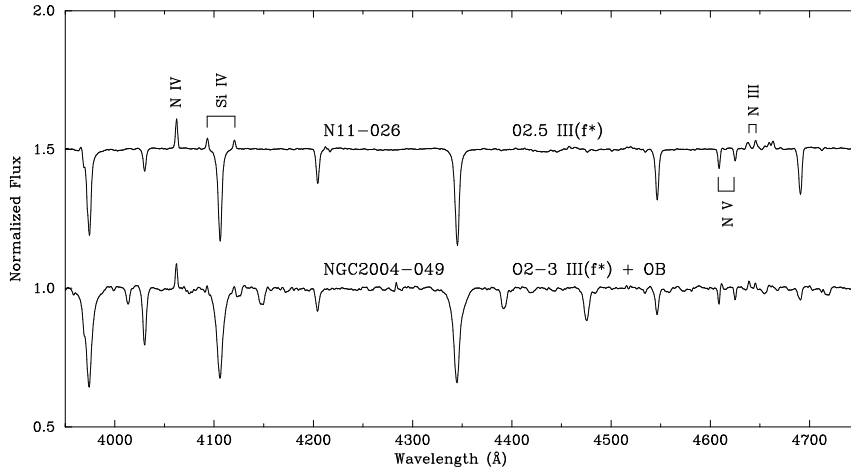


Fig. 5. Two early O-type stars: N11-026 and NGC 2004-049. The lines identified in N11-026 are, from left to right, N IV λ 4058; Si IV 4089-4116; N V λ 4604-4620; N III λ 4634-4640-4642. For clarity the spectra have been smoothed by a 1.5 Å FWHM filter.

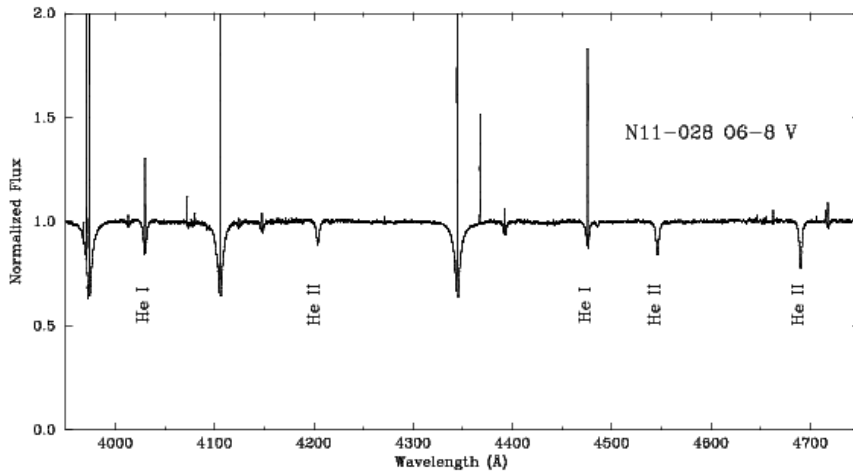


Fig. 6. The FLAMES spectrum of the principal star in N11A. The He II lines identified are, from left to right, λ 4200, 4542, 4686; the two strongest He I lines at λ 4026, 4471 are also labelled. Although the nebular spectrum somewhat dominates, there is strong absorption seen in both He I lines, necessitating a later spectral type than that adopted by Parker et al. (1992). For clarity the spectrum has been smoothed using a 7-pixel median filter.

relative ratio of He I λ 4471 to He II λ 4542 also appears different in the P92 spectrum in comparison to the FLAMES data; although we see no evidence for binarity in our spectra, variability of this object cannot be ruled out.

N11-038 and AzV 75 are shown together in Figure 7. Note the very weak N IV emission feature in N11-038, also consistent with an early O-type classification. The stronger N III emission and weaker He II λ 4686 absorption in AzV 75 suggest a more luminous star than N11-038, and these are borne out by the brighter *V* magnitude (taking into account the different distances and reddening). However we argue that both stars fall into the same morphological bin, cf. the standards in Walborn & Fitzpatrick (1990).

5.9. N11-040

Classification of this spectrum was relatively difficult, resulting in a final type of B0: III_n. There is apparent emission at the edge of both wings in the H α profile. There are also indications of binarity, with the He II lines appearing to have a slightly larger radial velocity than the other features, although the broadened lines make precise measurements very difficult.

5.10. N11-045

Classified here as O9-9.5 III, the hydrogen and helium spectrum of N11-045 is very similar to that of ι Ori (O9 III) from Walborn & Fitzpatrick (1990). However, we do not rule out a later O9.5 type; very weak Si III absorption is seen and the Si IV

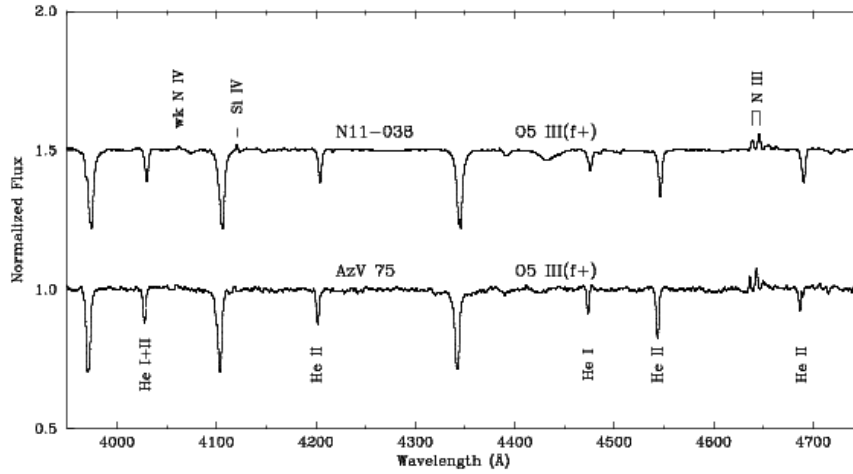


Fig. 7. The FLAMES spectrum of N11-038 compared with that of AzV 75 in the SMC, taken from Walborn et al. (2000). The lines identified are the same as in Figures 5 and 6. For clarity the spectra have been smoothed by a 1.5 \AA FWHM filter.

lines are slightly stronger than one would expect at O9, especially when one considers the reduced metallicity of the LMC.

5.11. NGC 2004-049

The spectrum of NGC 2004-049 is shown in Figure 5 and is classified here as O2-3 III(f*)+OB; the spectrum is very similar to that of LH10-3209 (Parker et al. 1992; Walborn et al. 2002). The N IV emission has a greater intensity than the N III lines, necessitating an early type of O2-3 for the primary. The secondary component in NGC 2004-049 appears cooler than in LH10-3209, with the He I $\lambda 4471$ absorption greater than that from He II $\lambda 4542$. Given the relatively weak He II $\lambda 4686$ in the composite spectrum, one can speculate there the secondary does not contribute significantly to this line and that the companion is of early B-type.

5.12. NGC 2004-057

Some $5'$ east of the cluster, NGC 2004-057 (Brey 45; Breysacher 1981) is a Wolf-Rayet star classified as WN4b by Smith et al. (1996), in which the ‘b’ denotes broad emission at He II $\lambda 4686$. Given the broad nature of the emission features, and the relatively short spectral range of each Giraffe wavelength-setting, it is not possible to rectify the data for NGC 2004-057 reliably. However, we retain the star in Table 7 as it highlights interesting objects found in the field. The FLAMES data appear to reveal small changes in the structure of emission lines such as He $\lambda 4542$, perhaps indicative of wind variability.

6. Emission-line stars

6.1. Be-type stars

The $H\alpha$ profile of NGC 346-023 has asymmetric, double-peaked emission, with infilling in the other Balmer lines. The absorption spectrum suggests a fairly hot star and is classified

as B0.2. Of particular note are numerous Fe II emission lines, together with emission from other metallic species, e.g. Mg II ($\lambda 4481$) and Si II ($\lambda\lambda 6347, 6371$). The $\lambda 4300$ to $\lambda 4700 \text{ \AA}$ region of its spectrum is shown in Figure 8. Permitted emission lines from Fe II are a well-known phenomenon in some Be-type stars (e.g. Wellmann 1952; Slettebak 1982), with more than a dozen found in the Magellanic Clouds by Massey et al. (1995). The most striking example of these stars in the FLAMES survey is NGC 346-023. Also shown in Figure 8 is another example, NGC 346-060, in which twin-peaked emission lines are seen, likely indicating a different viewing angle. Spectra with Fe II in emission are identified in Tables 4, 5, 6, and 7 as ‘Be-Fe’. The interesting Oe-type star, N11-055 (see Section 6.3) is also shown in Figure 8.

Prompted by the recent study in NGC 2004 by Martayan et al. (2006) we measured the equivalent widths of $H\alpha$ emission, $EW(H\alpha)$, for each of the Be-type FLAMES spectra. These values were then compared with the presence or absence of Fe II emission. Given the problems of nebular subtraction with multi-fibre data (which introduces a variable uncertainty, proscribing precise measurements in Be-type stars), we do not tabulate the $EW(H\alpha)$ values, and limit ourselves to a general discussion of the results. Hanuschik (1987) reported $EW(H\alpha) = 7 \text{ \AA}$ as the minimum for Fe II to be seen in Galactic Be stars. With the lower metallicity in the Clouds one might expect to find that the $EW(H\alpha)$ threshold for Fe II emission increases. Martayan et al. (2006) find that Fe II emission is seen in their LMC targets when $EW(H\alpha) > 20 \text{ \AA}$, with the inference that this higher threshold reflects the metallicity difference.

In our NGC 346 and NGC 330 fields we find the threshold for Fe II emission is $EW(H\alpha) > 15\text{-}20 \text{ \AA}$, above which Fe II emission is seen in all stars (except in NGC 346-045). Below this threshold Fe II emission lines are not seen except in NGC 330-031 [$EW(H\alpha) = 8.5 \text{ \AA} (\pm 1)$] which has very weak Fe II emission at $\lambda\lambda 4549, 4556, \text{ and } 4584$. Five of the six Be stars in N11 have Fe II emission lines (N11-056 is the exception

with very weak, double-peaked $H\alpha$ emission). Four of these five stars have $EW(H\alpha) > 20 \text{ \AA}$, with the fifth, N11-078, having $EW(H\alpha) \sim 4 \text{ \AA}$ (although as in NGC 330-031, the Fe II features are very weak). Lastly, in NGC 2004 both NGC 2004-023 and NGC 2004-035 have strong (i.e. $EW > 20 \text{ \AA}$) $H\alpha$ emission, accompanied by Fe II. Again we find one star (NGC 2004-025) with $EW(H\alpha)$ below 20 \AA (in this case ~ 12.5) with very weak Fe II emission.

In summary, Fe II is seen in emission in most stars for which $EW(H\alpha) > 15 \text{ \AA}$; a strong $H\alpha$ emission profile does not guarantee Fe II emission, but it is very probable. Also, the threshold isn't completely exclusive, below it we see weak (but clear) emission in the stronger Fe II lines in three stars. Following this investigation of the LMC and SMC spectra, we revisited the 12 Be-type stars from Paper I to check for Fe II emission. In Paper I we did not pay particular attention to Fe II emission, apart from in the Herbig-type star 6611-022. In fact, there are three stars from Paper I with $EW(H\alpha) > 20 \text{ \AA}$ (3293-011, 4755-014, and 4755-018) and Fe II emission is seen in each of these. There are two further stars with moderate $H\alpha$ emission, 6611-010 and 6611-028, for which $EW(H\alpha) = 15.5$ and $13.5 (\pm 1)$ respectively. There appears to be very weak Fe II emission in both of these spectra, analogous to the stars with moderate $H\alpha$ emission in our LMC and SMC sample. The weak emission in 6611-010 (W503, Walker 1961) was also noted by Hillenbrand et al. (1993), leading to their classification of the spectrum as a Herbig-type object.

With the benefit of new instrumentation and detectors we can detect Fe II emission that may have gone un-noticed previously. It seems clear that irrespective of environment, if $EW(H\alpha) > 20 \text{ \AA}$, it is very probable that Fe II emission will also be observed. The statement from Hanuschik (1987) was that 'one should not expect to find *notable* amounts of Fe II emission for stars with $EW(H\alpha) < 7 \text{ \AA}$.' This remains true and, if anything, should be revised upwards slightly, depending on one's definition of 'notable.' However, we dispute the claim by Martayan et al. (2006) that their observations in NGC 2004 display the expected offset arising from the lower metallicity - although we have not measured the intensity of the Fe II emission, we see no obvious trend with metallicity for the *presence* of Fe II emission.

Given that both NGC 346 and N11 are relatively young regions it does suggest the question of whether these stars are classical Be-type stars, or are they associated with younger (pre-main-sequence) objects. Indeed, the cores of both regions are younger than the 10 Myr threshold given by Fabregat & Torrejon (2000) for classical Be-type stars to form.

In NGC 346 the three Be-Fe stars closest to the centre of the cluster are NGC 346-023, 036 and 065, all of which are on the periphery of the central ionized region (see Figure 13). Similarly in N11, the Be-Fe stars are not in the obviously dense star-forming regions. Given that also we find such stars in the NGC 2004 and NGC 330 pointings (that sample the more general field population) it seems most plausible that the Be-Fe stars are associated with classical Be-types, rather than younger objects. However, it should be noted that Mokiem et al. (2006) find evidence for coeval O-type stars beyond the ionized region in NGC 346 - detailed analysis of the Be-Fe stars is required

to test whether those in the NGC 346 field are actually coeval with the young O-stars, or whether they are older.

6.2. Shell stars

In Figure 9 we show the spectrum of NGC 346-048, which permits an elegant comparison with NGC 346-023. The $H\alpha$ profile of NGC 346-048 is double-peaked, leading to moderate 'shell' effects in the $H\gamma$ line shown in Figure 9. Such a spectrum is thought to originate from absorption by a cooler disk in front of the star (e.g. Hanuschik 1995; Hummel & Vrancken 2000) and also leads to the Fe II absorption seen in the figure, uncharacteristic of a star classified as B3-type and more comparable to those seen in the sharp-lined, A0 II spectrum of NGC 346-014. Note the weak emission in the wings of the $\lambda 4584$ Fe II line in NGC 346-048. Similar absorption from Fe II is also seen in NGC 330-093, although the signal-to-noise of the data is lower given the fainter magnitude of the star.

6.3. Oe-type stars

6.3.1. N11-055: An 'Oe-Fe' star

This star has a very complex spectrum, a section of which is shown in Figure 8. Emission is seen in all of the observed Balmer lines, and most of the He I lines are infilled by a twin-peaked profile (e.g. $\lambda 4026$), with the $\lambda 4713$ line seen solely in (twin-peaked) emission. A large number of Fe II emission lines are also seen. We find no strong evidence for binarity, with all the features apparently consistent with one radial velocity; the mean radial velocity from the 3 He II lines is 293 km s^{-1} . We classify the star here as O7-9 IIIne, with the uncertainty in spectral type arising due to the significant infilling in the He I lines. Assuming that there is no significant companion, the intensity of the $\lambda 4200$ and $\lambda 4542$ He II lines suggests that the later-type is most likely the best description of the spectrum. Also, the He II $\lambda 4686$ line appears too weak for the star to be classified as a dwarf, hence the adoption of class III.

In a sense, this star appears as a much less extreme version of iron stars such as HD 87643 (Walborn & Fitzpatrick 2000). However, the iron stars tend to show strong P Cygni features in some of their lines, which are not seen here. The $H\alpha$ emission in N11-055 is strong and symmetric, suggesting this star might be more closely related to Be-type stars, with HD 155806 a likely Galactic counterpart (Walborn 1980).

6.3.2. NGC 346-018

NGC 346-018 (MPG 217) is classified as O9.5 IIIe. The spectrum displays very strong and broad $H\alpha$ emission, with the higher-order lines of the Balmer series somewhat in-filled. The He I $\lambda 6678$ line is strongly in emission and there is evidence of significant infilling in He I $\lambda 4471$ (and perhaps other He I lines in the blue region); we have taken this into account when classifying the spectrum, as discussed by Negueruela et al. (2004).

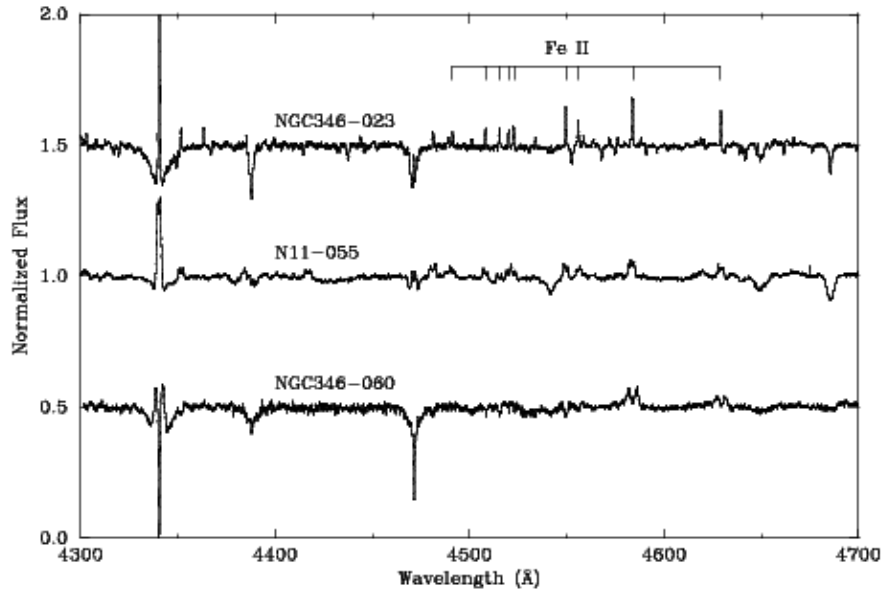


Fig. 8. Examples of Be/Oe-type spectra with Fe II emission lines. The Fe II lines identified in NGC 346-023 are $\lambda\lambda$ 4491, 4508, 4515, 4520, 4523, 4549, 4556, 4584, and 4629. For clarity the spectra have been filtered by a 7-pixel median filter and to ease the comparison between SMC and LMC spectra they are corrected for their tabulated radial velocities to rest wavelengths.

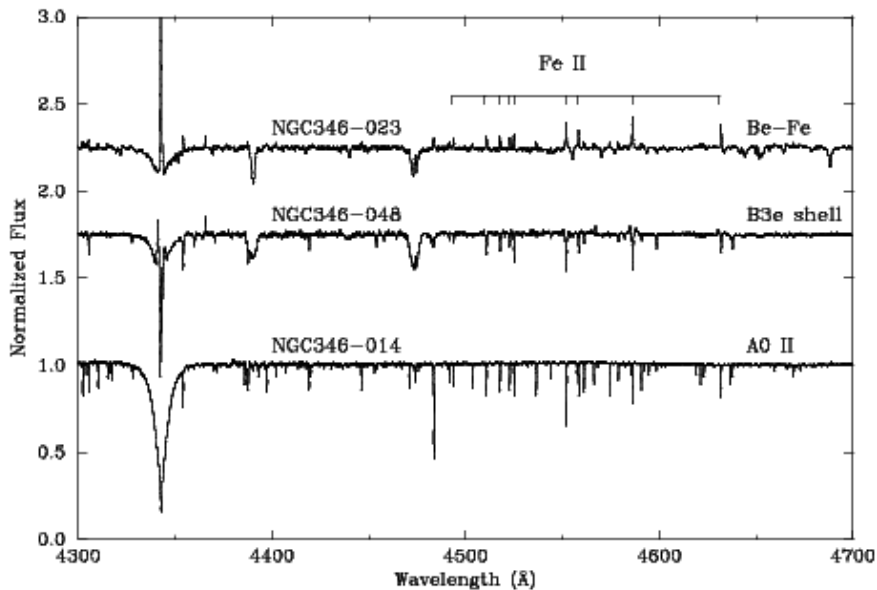


Fig. 9. A comparison of Be-type stars with Fe II emission and absorption lines. The Fe II lines identified are the same as in Figure 8, and the spectra have also been filtered by a 7-pixel median filter. The spectrum of NGC 346-014 is included to highlight that the Fe II lines are indicative of a much cooler temperature, comparable to that seen in early A-type stars.

6.3.3. NGC 330-023

The spectrum of NGC 330-023 has strong, broad $H\alpha$ emission, with an equivalent width of $28 \pm 3 \text{ \AA}$ (with the uncertainty arising from the rectification in the wings of the emission). It's conceivable that part of this emission may be nebular in origin, but the absence of [N II] emission suggests that the majority is intrinsic to the star. The blue-region spectrum is particularly interesting, with He II absorption lines consistent with a late O-

type star. It is difficult to assign a precise classification due to significant infilling of the He I lines; however from intensity of the He II lines we classify the star as approximately O9-type. Of note (see Figure 10) is the twin-peaked emission seen in both He I $\lambda\lambda$ 471 and 4713. The luminosity class is harder to ascertain, with a final classification of O9 V-IIIe adopted.

Prior to the new HR03 spectra obtained in 2005, radial velocity measurements were limited to the three He II lines, with

a mean value of 159 km s^{-1} (with standard deviation, $\sigma = 10$), and with two of the lines included in the same wavelength setting. Inspection of the spectra acquired in 2005 reveal significant variations in the asymmetric $\text{H}\delta$ emission feature, as shown in Figure 11. With no obvious radial velocity shifts seen in other lines, such differences resemble the V/R (violet / red) variability seen in Be-type stars, suggested by Hanuschik et al. (1995) as arising from oscillations in the disk. Hummel et al. (2001) studied Be-type stars in NGC 330 to see if this phenomenon was metallicity dependent as theory would suggest, but found that the fraction of stars undergoing disk oscillations was comparable to that in Galactic targets. We note that NGC 330-023 is the photometric variable #95V reported by Sebo & Wood (1994), with the variability presumably arising from changes such as those reported here.

7. Compilation of previous spectroscopy

For completeness, in Table 8 the FLAMES classifications presented here are compared with previous types. Published classifications are included from: W77 (Walborn 1977); FB80 (Feast & Black 1980); CJF85 (Carney et al. 1985); NMC (Niemela et al. 1986); G87 (Garmany et al. 1987); MPG (Massey et al. 1989); F91 (Fitzpatrick 1991); P92 (Parker et al. 1992); L93 (Lennon et al. 1993); M95 (Massey et al. 1995); G96 (Grebel et al. 1996); HM00 (Heydari-Malayeri et al. 2000); W00 (Walborn et al. 2000); L03 (Lennon et al. 2003); EH04 (Evans et al. 2004). Note that we do not include published types from objective-prism spectroscopy, preferring to limit our comparisons to long-slit/multi-object observations.

With the benefit of the high-quality FLAMES spectra, many of the classifications from Evans et al. (2004) are now refined. There are few significant differences between the FLAMES classifications and those extant in the literature. Two stars (N11-028 and N11-038) have already been discussed in Section 5 – one further target worthy of comment is N11-080 which appears to be comprised of two late-type O stars from the FLAMES data, compared to the O4-6 V classification from P92. This is not surprising given that P92 had noted the spectrum as a possible composite object.

8. Discussion

In Table 2 we give an overview of the entire sample in the FLAMES survey, incorporating the LMC and SMC observations reported here, with the Galactic data from Paper I. Analysis of many of these data is now well advanced by different groups. Here, with the benefit of a broad view of the whole sample, we discuss some of the more general features of the survey.

8.1. H-R diagrams for each of the fields

In Figure 12 we show Hertzsprung-Russell (H-R diagrams) for each of our LMC and SMC fields. These have been compiled by employing various published calibrations – clearly the detailed studies of different subsets of the survey will yield precise determinations of temperatures and luminosities, but

we take the opportunity now to show the full extent of the LMC/SMC stars in the H-R diagram. Objects listed as likely foreground objects are plotted as open circles, likely binaries as '+', and emission-line objects as triangles. For illustrative purposes the evolutionary tracks shown are from Schaerer et al. (1993) for the LMC targets and from Charbonnel et al. (1993) for the SMC.

Temperatures were adopted on the basis of spectral type, luminosity and metallicity from Massey et al. (2005, O-type stars), Crowther et al. (2006, B-type supergiants), Evans & Howarth (2003, A-type supergiants), and Schmidt-Kaler (1982, for other types). Objects that luminosity classes of III or V were assigned temperatures from calibrations for dwarfs; more luminous stars (i.e. II, Ib, Iab and Ia) adopted temperatures from calibrations of supergiants. With no metallicity-dependent temperature scale in the literature for early B-type supergiants, temperatures were taken from the Galactic results (Crowther et al. 2006), which were found to be in good agreement with those from analysis of individual stars in the SMC (Trundle et al. 2004; Trundle & Lennon 2005).

Luminosities were calculated using intrinsic colours from Fitzgerald (1970), extrapolating or interpolating where required; bolometric corrections were calculated using the relations from Vacca et al. (1996) for the earliest types, and from Balona (1994) for the cooler stars; the ratio of total to selective extinction (R) in the LMC was taken as 3.1 (e.g. Howarth 1983) and as 2.7 in the SMC (Bouchet et al. 1985); distance moduli were taken as 18.5 to the LMC (e.g. Gibson 2000) and 18.9 to the SMC (Harries et al. 2003).

Figure 12 highlights the predominantly less-massive populations observed in the two older clusters (i.e. NGC 2004 and NGC 330), particularly when compared to N11. The N11 observations also sample a more luminous, more massive population than those in NGC 346. This is, in part, influenced by the fact that some of the O-type stars observed by Walborn et al. (2000) were explicitly avoided in the FLAMES survey as state-of-the-art analyses have already been presented in the literature (e.g. Bouret et al. 2003).

8.2. Exploring new regions of N11

As mentioned earlier, part of our intention in the FLAMES observations was to explore some of the less dense, apparently star-forming regions in N11. In addition to the discovery of the O2.5-type star to the north of LH10, the survey has revealed a large number of O-type stars in the regions surrounding LH9 and LH10. In Figure 17 we show the V -band WFI image used for target selection in N11, with the O- and B-type stars marked in different colours; LH9, LH10 and LH13 are also identified in the image. Note the O-type stars to the south of LH9, newly discovered by this survey. These include N11-020 [classified as O5 I(n)fp] on the northern edge of the N11F region (cf. Figure 15).

Furthermore, N11-004 [O9.7 Ib] is the bright star in N11G, and N11-058 [O5.5 V((f))] is one of two visually bright stars in N11I, the other being N11-102 [B0.2 V]. Both N11G and N11I appear as small 'bubbles' in near-IR images, presumably driven

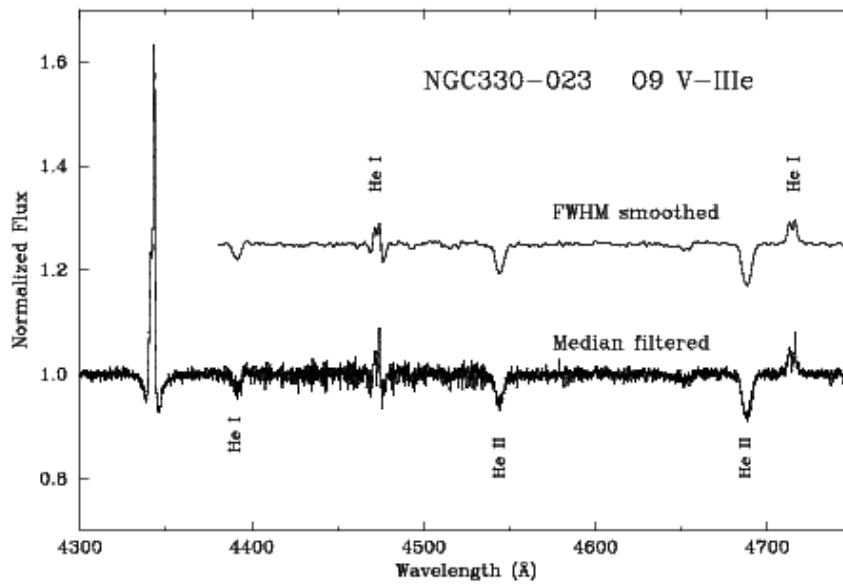


Fig. 10. A section of the blue-region spectrum of NGC 330-023, highlighting the double-peaked emission in the He I lines at $\lambda 4471$ and $\lambda 4713$. The lower spectrum is at full-resolution, but has been filtered to remove cosmic rays using a 7-pixel median filter. The upper spectrum has been smoothed with a 1.5 \AA FWHM filter. The lines marked in the lower spectrum are He I $\lambda 4388$, and He II $\lambda \lambda 4542, 4686$.

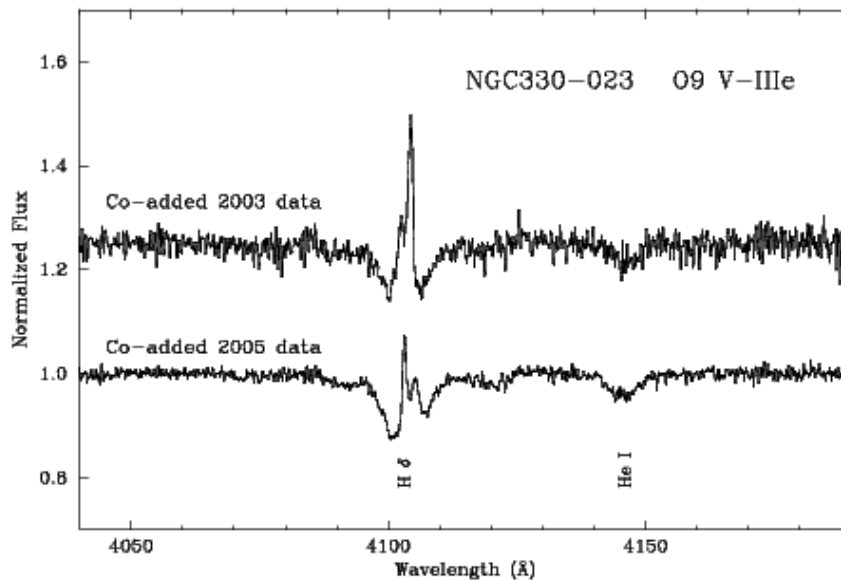


Fig. 11. Co-added spectra of NGC 330-023 from the two epochs of HR03 observations. Both spectra have been 7-pixel median filtered for clarity. Note the change in structure of the emission at $H\delta$, and the apparent wavelength invariance of the (albeit broadened or infilled) He I $\lambda 4143$ line.

by the ionization and/or the stellar winds from these stars. We have also observed N11-029 [OC9.7 Ib] in N11H, which appears radially smaller than N11G and N11I.

The densest regions in N11, i.e. N11B (LH10) and N11C (LH13) have been demonstrated by other authors (Parker et al. 1992; Walborn & Parker 1992; Heydari-Malayeri et al. 2000; Barbá et al. 2003) to have rich, young populations of early-type stars. The general consensus is that this region is a two-stage starburst, with the evolution of LH9 triggering star-formation

around it. For the first time the FLAMES survey has observed the regions to the south and west of LH9 – whilst much smaller in size and stellar content, we find newly discovered O-type stars as the likely source of ionization and dynamic energy for the observed nebulae.

To place this region in context, the ‘bigger picture’ is dramatically illustrated by the cover image of Edition #80 of the National Optical Astronomy Observatory/National Solar Observatory (NOAO/NSO) Newsletter. This features an im-

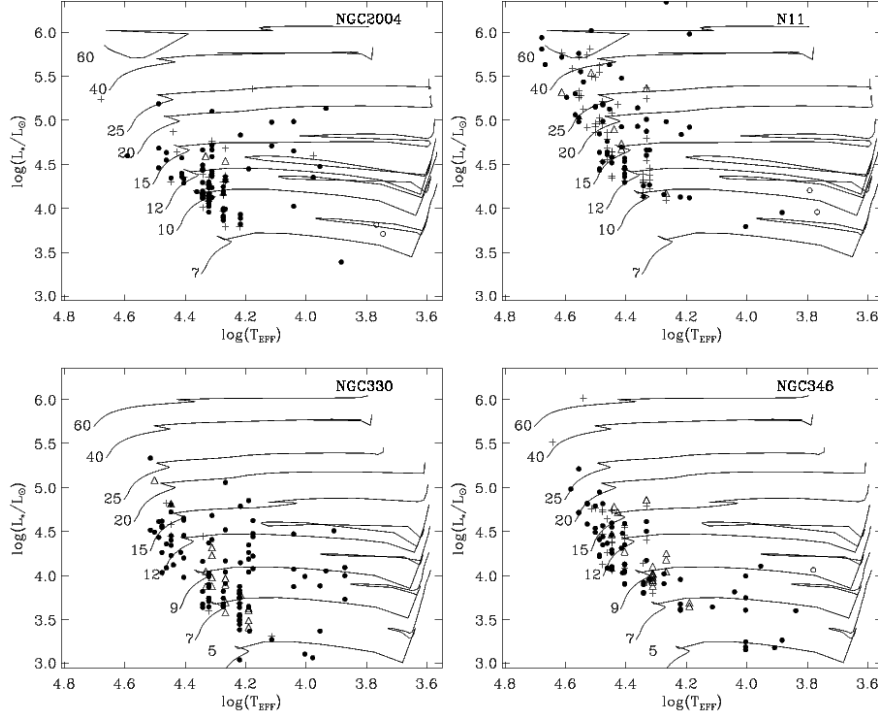


Fig. 12. H-R diagrams for the four FLAMES fields in the Magellanic Clouds. Open circles denote foreground stars, open triangles are emission-line objects, and likely binaries are indicated with crosses. The evolutionary tracks are taken from Schaerer et al. (1993) for N11 and NGC 2004, and from Charbonnel et al. (1993) for NGC 330 and NGC 346.

Table 2. Overview of the distribution of spectral types of the FLAMES survey, including the Galactic clusters from Paper I.

Field	O	Early-B (B0-3)	Late-B (B5-9)	AFG	Total
MW: ϕ NGC 3293	—	48	51	27	126
MW: ϕ NGC 4755	—	54	44	10	108
MW: ϕ NGC 6611	13	28	12	32	85
SMC: NGC 330	6	98	11	10	125
SMC: NGC 346	19	84	2	11	116
LMC: NGC 2004	4 (+ 1 WR)	101	6	7	119
LMC: N11	44	76	—	4	124
Total	87	489	126	101	803

age of N11 from the Magellanic Clouds Emission Line Survey (credited to Drs. S. Points, C. Smith, and M. Hanna). In addition to N12, N13, and N14, the image includes the significantly extended shell of gas that constitutes N10 from Henize (1956).

8.3. ‘Blue stragglers’ in NGC 330

Blue stragglers were reported in NGC 330 by Lennon et al. (1993), with Grebel et al. (1996) arguing that they might be a product of binary evolution. Blue stragglers are thought to arise from either mass-exchange or stellar mergers (e.g. Pols & Marinus 1994), with recent studies of globular clusters suggesting that both channels play a role (Davies et al. 2004).

Six of our targets in the NGC 330 observations are late O-type stars, three of which are less than $5'$ from the centre of the cluster: NGC 330-023 (see Section 6.3.3), NGC 330-049, and NGC 330-123.

In particular, NGC 330-123 (R74-B18) is classified here as O9.5 V, cf. B0 Ve from Lennon et al. (1993) and O9 III/Ve from Grebel et al. (1996, who were quoting unpublished types from Lennon). Narrow (and weak) emission is seen in the core of the $H\alpha$ Balmer line in the UVES spectrum of NGC 330-123, but is accompanied by [N II] emission so the origins are likely nebular. Indeed, Keller & Bessell (1998) note that there is an elliptical region of diffuse nebular emission centred on this star, it would appear that NGC 330-123 is the ionization source of

this nebulosity. Interestingly, the radial velocity of NGC 330-123 is 177 km/s (with standard deviation, $\sigma = 5$), i.e. different from the systemic velocity of the cluster which is ~ 155 km/s (e.g. Lennon et al. 2003). Binariness is a possible explanation of this difference, but additional spectra at other epochs (October 1992 and October 1995), though of lower resolution, are in good agreement with the FLAMES data. If this star is coeval with the cluster then its current radial velocity might indicate a previous, though relatively recent ejection event. Its radial velocity however is similar to the three more distant O-type stars in the NGC 330 field: NGC 330-013, NGC 330-046 and NGC 330-052, which have $v_r = 176, 177$ and 166 km s⁻¹ respectively. Two of these, NGC 330-013 and NGC 330-052, are found to be helium rich (Mokiem et al. 2006), whilst NGC 330-123 has also been reported as helium rich by Lennon et al. (1993, note that this paper erroneously refers to R74-A01 as helium rich, when it should actually refer to R74-B18, i.e. NGC 330-123). All four stars could perhaps be considered as members of the general field population which, from the H-R diagram (Figure 12), can be seen to extend well beyond the notional cluster turn-off – as represented by the ~ 20 stars with spectral types earlier than B1. We note that the majority of these stars have radial velocities rather different from the cluster radial velocity, suggesting that the probable number of true blue stragglers in this field belonging to NGC 330 is small.

Both NGC 330-023 and NGC 330-049 are late O-type stars with velocities consistent with the cluster (cf. Lennon et al. 2003), although the peculiarities of NGC 330-023 have already been discussed in Section 6.3.3. At respective radial distances of 2.3' and 4.5' they are not immediately proximate to the cluster core, but are perhaps outer members of the cluster and therefore could be true blue stragglers.

The situation for NGC 2004 is qualitatively similar to that of NGC 330. The Wolf-Rayet and O2-3 stars stand out as potential blue stragglers but are more likely field stars, though the presence of an O2-3 star in the field is unusual in itself. One further candidate blue straggler is NGC 2004-019, which is close to the core, with $r_d = 1.5'$.

8.4. Incidence of Be-stars

The numbers of Be-type stars in each FLAMES pointing are summarised in Table 3. The observed field-population of B- and Be-type stars in our NGC 330 and NGC 2004 pointings should be relatively unaffected by specific selection effects (Section 2.4), aside from the slightly different ($\sim 0.5^m$) faint cut-off of the observations.

The Be-stars in Table 3 include some in the outer regions of the clusters themselves. As an experiment, we considered the B-type stars with $r_d > 2'$ in NGC 330 and NGC 2004 to sample the field population away from the main clusters. All stars in the range B0-3 were counted and then the relative percentage of those that are seen to be Be-type stars was found. In NGC 2004 this ratio for the field population (i.e. Be / [Be+B]) was 16% (13/81), compared to 23% (18/77) in NGC 330. It is difficult to quantify the uncertainties in these results. Is there any effect in terms of absolute magnitude? As a further ex-

periment (and still with the $r_d > 2'$ condition) we considered the early B-type stars in our NGC 330 data with $V \leq 16.03$. Taking the difference of the distance moduli of the Clouds as 0.4^m , and allowing for the fact that the ‘typical’ extinction toward the LMC is $\sim 0.1^m$ greater than the SMC (Massey et al. 1995), this notionally imposes a similar cut-off as that in the NGC 2004 data. The Be-fraction for the NGC 330 field population remains robust at 24% (11 Be/45 Be+B).

Our results are in reasonable agreement with those from Keller et al. (1999) and, for NGC 2004, match those of Martayan et al. (2006). Both Keller et al. and Martayan et al. advanced their results as a lack of evidence for a strong dependence of the Be-fraction with metallicity when compared to the general result for the Milky Way of ~ 17 -20% (Zorec & Briot 1997). This is in contrast to the results for clusters from Maeder et al. (1999). The statistics in our NGC 346 and N11 data do not provide a meaningful test of the relative numbers of Be stars at different metallicities. Aside from a likely mix of field and cluster populations in the NGC 346 pointing, the N11 region is even less suited given its complex star-formation history.

8.5. Binaries and the binary fraction

With the time-sampling provided by the service-mode observations we are reasonably sensitive to detection of binarity in our SMC and LMC targets. In Appendix A we give full details of the observational epochs of the FLAMES spectra. The observations in both N11 and NGC 2004 spanned a total of 57 days, and those in NGC 346 covered 84 days. The time-coverage of the majority of the NGC 330 data is not as extensive as for the other fields, covering 10 days. The new HR03 ($\lambda 4124$) data offer some extra information in this regard (e.g. Section 6.3.3). However, given the relatively poor signal-to-noise in the 2003 data it is difficult to compare measured velocities meaningfully – from these comparisons a number of stars are flagged as having potentially variable velocities.

The FLAMES data are sufficient to derive periods for some of the newly discovered systems, the most interesting of which will receive a detailed treatment in a future study. The incidence of binaries is summarised in Table 3. We stress that stars considered as multiple in this discussion are those listed in Tables 4, 5, 6, and 7 as ‘Binary’ (be they SB1, SB2 or not specified). Stars suggested to perhaps demonstrate v_r variations are not considered further, pending follow-up. As such, the percentages in Table 2 serve as strong, *lower* limits on the binary fraction in our fields.

In young, dense clusters multiplicity seems a common, almost ubiquitous feature. García & Mermilliod (2001) found a significant binary fraction (79%) in the very young Galactic cluster NGC 6231, and Weigelt et al. (1999) and Preibisch et al. (1999) highlighted the high degree of multiplicity found in the massive members of the Orion Nebula, suggesting a different mode of star formation to that at lower masses (in which the binary fraction is lower).

The formation mechanism of massive stars is still a point of significant debate. In their discussion of the competing

scenarios of massive-star formation from accretion versus stellar mergers, Bally & Zinnecker (2005) suggest that the multiple star fraction will be larger if merging dominates. Bally & Zinnecker also suggest that mergers may be the dominant process in ultradense regions such as 30 Doradus; perhaps the high binary fraction of O- and early B-type stars in N11 is indicative of this mode of star-formation, remembering that 36% is a solid, lower limit obtained from a programme that was not optimised for detection of binaries.

By comparison, the low binary fraction in the NGC 330 targets is somewhat puzzling. Although fewer binaries are generally found in the field population (e.g. Mason et al. 1998), the NGC 330 fraction is significantly lower than that for NGC 2004, which similarly samples the field (see Figures 14 and 16). We speculate that, whilst the new HR03 data added an additional epoch to the time-sampling for the NGC 330 targets, it is still not as thorough as for the other fields.

9. Summary

Quantitative analyses of different subsets of the FLAMES survey are now underway by various groups, e.g. Dufton et al. (submitted); Hunter et al. (submitted); Mokiem et al. (2006). Here we have presented a significant dataset of high-resolution observations of early-type stars in the Magellanic Clouds, giving stellar classifications and radial velocities, and noting evidence of binarity from the multi-epoch observations. Spectral peculiarities were discussed, in particular with regard to emission-line spectra. We have found a relatively large number of Be-type stars that display permitted Fe II emission lines. We find that in nearly all the spectra with $EW(H\alpha) > 20 \text{ \AA}$, Fe II is seen in emission. We do not find evidence for a metallicity-dependent scaling of the required $H\alpha$ equivalent width for Fe II emission to be present, contrary to the suggestion by Martayan et al. (2006). We have tentatively explored the relative fraction of Be- to normal B-type stars in the field-regions of NGC 330 and NGC 2004, finding no compelling evidence of a strong trend with metallicity *for field stars*.

We have investigated previously unexplored regions around the central LH9/LH10 complex of N11, finding ~ 25 new O-type stars from our spectroscopy. Furthermore, to the north of LH10 we have discovered a very hot, potential runaway star (N11-026) that we classify as O2.5 III(f*).

For three of our fields we find lower limits to the binary fraction of O- and early B-type stars of 23 to 36%. Following identification of a relatively large number of binaries, more sophisticated methods will be used in a subsequent paper to characterise as many of these systems as possible. NGC 346-013 is particularly interesting with an apparently hotter, more massive, but less luminous secondary component.

The overall distribution of the targets observed in the VLT-FLAMES survey of massive stars is summarised in Table 2. The large number of O-type stars observed will provide allow for better sampling of this domain, building on the significant studies by Massey et al. (2004, 2005). In the early B-type domain the FLAMES survey is truly unique, allowing precise abundance determinations of a hitherto impossible number of stars (Hunter et al., submitted), enabling us to really address

some of the unsolved questions regarding the dependence of stellar evolution on metallicity.

Acknowledgements: We are very grateful to Francesca Primas and the staff at Paranal for their invaluable assistance with the observational programme, and to Nolan Walborn for his comments on the manuscript. We also thank Mike Irwin for processing the N11 and NGC 2004 images, and Andreas Kaufer for reducing the FLAMES-UVES data. Finally we thank the referee, Dr. Anne-Marie Hubert, for her useful comments & suggestions. CJE acknowledges financial support from the UK Particle Physics and Astronomy Research Council (PPARC) under grant PPA/G/S/2001/00131, and the continued support of the other members of the FLAMES massive star consortium. SJS acknowledges support from the EURYI scheme.

References

- Ardeberg, A., Brunet, J. P., Maurice, E., & Prevot, L. 1972, *A&AS*, 6, 249
- Arp, H. C. 1959, *AJ*, 64, 254
- Azzopardi, M. & Vigneau, J. 1975, *A&AS*, 22, 285
- Azzopardi, M. & Vigneau, J. 1982, *A&AS*, 50, 291
- Ballester, P., Boitquin, O., Modigliani, A., & Wolf, S. 2004, *UVES Pipeline User Manual*, 2nd edn.
- Bally, J. & Zinnecker, H. 2005, *AJ*, 129, 2281
- Balona, L. A. 1994, *MNRAS*, 268, 119
- Balona, L. A. & Jerzykiewicz, M. 1993, *MNRAS*, 260, 782
- Barbá, R. H., Rubio, M., Roth, M. R., & García, J. 2003, *AJ*, 125, 1940
- Bencivenni, D., Brocato, E., Buonanno, R., & Castellani, V. 1991, *AJ*, 102, 137
- Bertrand, J.-F., St-Louis, N., & Moffat, A. F. J. 1998, in *Boulder-Munich II: Properties of Hot, Luminous Stars*, ed. I. D. Howarth (ASP Conference Series vol. 131, San Francisco), 376
- Blaauw, A. 1961, *Bull. Astron. Inst. Netherlands*, 15, 265
- Blecha, A., North, P., Royer, F., & Simond, G. 2003, *BLDR Software - Reference Manual*, 1st edn.
- Bouchet, P., Lequeux, J., Maurice, E., Prevot, L., & Prevot-Burnichon, M. L. 1985, *A&A*, 149, 330
- Bouret, J.-C., Lanz, T., Hillier, D. J., et al. 2003, *ApJ*, 595, 1182
- Breysacher, J. 1981, *A&AS*, 43, 203
- Carney, B. W., Janes, K. A., & Flower, P. J. 1985, *AJ*, 90, 1196
- Charbonnel, C., Meynet, G., Maeder, A., Schaller, G., & Schaerer, D. 1993, *A&AS*, 101, 415
- Crowther, P. A., Hillier, D. J., Evans, C. J., et al. 2002, *ApJ*, 579, 774
- Crowther, P. A., Lennon, D. J., & Walborn, N. R. 2006, *A&A*, 446, 279
- Davies, M. B., Piotto, G., & de Angeli, F. 2004, *MNRAS*, 349, 129
- Evans, C. J. & Howarth, I. D. 2003, *MNRAS*, 345, 1223
- Evans, C. J., Howarth, I. D., Irwin, M. J., Burnley, A. W., & Harries, T. J. 2004, *MNRAS*, 353, 601

Table 3. Overview of the number of Be-type stars and binaries in the LMC and SMC sample

Field	O (+ Oe)	Early-B (B0-3)	Be	Total (O+Early- B)	Binary Fraction
SMC: NGC 330	6	76	22	104	
<i>Binary</i>	–	3	1	4	4%
SMC: NGC 346	19	59	25	103	
<i>Binary</i>	4	19	4	27	26%
LMC: NGC 2004	4	83	18	105	
<i>Binary</i>	1	21	2	24	23%
LMC: N11	44	68	8	120	
<i>Binary</i>	19	21	3	43	36%

- Evans, C. J., Smartt, S. J., Lee, J.-K., et al. 2005, *A&A*, 437, 467, (Paper I)
- Fabregat, J. & Torrejon, J. M. 2000, *A&A*, 357, 451
- Feast, M. W. 1972, *MNRAS*, 159, 113
- Feast, M. W. & Black, C. 1980, *MNRAS*, 191, 285
- Fitzgerald, M. P. 1970, *A&A*, 4, 234
- Fitzpatrick, E. L. 1988, *ApJ*, 335, 703
- Fitzpatrick, E. L. 1991, *PASP*, 103, 1123
- García, B. & Mermilliod, J.-C. 2001, *A&A*, 122, 136
- Garmany, C. D., Conti, P. S., & Massey, P. 1987, *AJ*, 93, 5
- Gibson, B. K. 2000, *Mem. Soc. Astron. Ital.*, 71, 693
- Grebel, E. K., Richtler, T., & de Boer, K. S. 1992, *A&A*, 254, 5
- Grebel, E. K., Roberts, W. J., & Brandner, W. 1996, *A&A*, 311, 470
- Hanuschik, R. W. 1987, *A&A*, 173, 299
- Hanuschik, R. W. 1995, *A&A*, 295, 423
- Hanuschik, R. W., Hummel, W., Dietle, O., & Sutorius, E. 1995, *A&A*, 300, 163
- Harries, T. J., Hilditch, R. W., & Howarth, I. D. 2003, *MNRAS*, 339, 157
- Henize, K. G. 1956, *ApJS*, 2, 315
- Heydari-Malayeri, M., Charmandaris, V., Deharveng, L., et al. 2001, *A&A*, 372, 527
- Heydari-Malayeri, M., Royer, P., Rauw, G., & Walborn, N. R. 2000, *A&A*, 361, 877
- Heydari-Malayeri, M. & Testor, G. 1985, *A&A*, 144, 98
- Hillenbrand, L. A., Massey, P., Strom, S. E., & Merrill, K. M. 1993, *AJ*, 106, 1906
- Howarth, I. D. 1983, *MNRAS*, 203, 301
- Hummel, W., Gässler, W., Muschelok, B., et al. 2001, *A&A*, 371, 932
- Hummel, W. & Vrancken, M. 2000, *A&A*, 359, 1075
- Irwin, M. J. & Lewis, J. 2001, *NewAR*, 45, 105
- Israel, F. P. & Koornneef, J. 1991, *A&A*, 248, 404
- Keller, S. C. & Bessell, M. S. 1998, *A&A*, 340, 397
- Keller, S. C., Wood, P. R., & Bessell, M. S. 1999, *A&AS*, 134, 489
- Korn, A. J., Daflon, S., Nieva, M. F., & Cunha, K. 2005, *A&A*, 633, 899
- Korn, A. J., Keller, S. C., Kaufer, A., et al. 2002, *A&A*, 385, 143
- Kudritzki, R.-P., Cabanne, M. L., Husfeld, D., et al. 1989, *A&A*, 226, 235
- Lennon, D. J. 1997, *A&A*, 317, 871
- Lennon, D. J., Dufton, P. L., & Crowley, C. 2003, *A&A*, 398, 455
- Lennon, D. J., Mazzali, P. A., Pasian, P., Bonifacio, P., & Castellani, V. 1993, *SSRv*, 66, 169
- Lucke, P. B. & Hodge, P. W. 1970, *AJ*, 75, 171
- Maeder, A., Grebel, E. K., & Mermilliod, J.-C. 1999, *A&A*, 346, 459
- Martayan, C., Hubert, A.-M., Floquet, M., et al. 2006, *A&A*, 445, 931
- Mason, B. D., Gies, D. R., Hartkopf, W. I., et al. 1998, *AJ*, 115, 821
- Massey, P., Bresolin, F., Kudritzki, R.-P., Puls, J., & Pauldrach, A. W. A. 2004, *ApJ*, 608, 1001
- Massey, P., Lang, C. C., DeGioia-Eastwood, K., & Garmany, C. D. 1995, *ApJ*, 438, 188
- Massey, P., Parker, J. W., & Garmany, C. D. 1989, *AJ*, 98, 1305
- Massey, P., Puls, J., Pauldrach, A. W. A., et al. 2005, *ApJ*, 627, 477
- Mazzali, P. A., Lennon, D. J., Pasian, F., et al. 1996, *A&A*, 316, 173
- McGregor, P. J. & Hyland, A. R. 1984, *ApJ*, 277, 149
- Meyssonier, N. & Azzopardi, M. 1993, *A&AS*, 102, 451
- Mihalas, D. 1972, *ApJ*, 177, 115
- Mokiem, M. R., de Koter, A., Evans, C. J., et al. 2006, *A&A*, in press
- Momany, Y., Vandame, B., Zaggia, S., et al. 2001, *A&A*, 379, 436
- Morrell, N. I., Walborn, N. R., & Fitzpatrick, E. L. 1991, *PASP*, 103, 341
- Nazé, Y., Antokhin, I. I., Rauw, G., et al. 2004a, *A&A*, 418, 841
- Nazé, Y., Hartwell, J. M., Stevens, I. R., et al. 2003, *ApJ*, 586, 983

- Nazé, Y., Manfroid, J., Stevens, I. R., Corcoran, M. F., & Flores, A. 2004b, *ApJ*, 608, 208
- Negueruela, I., Steele, I. A., & Bernabeu, G. 2004, *Astron. Nachr.*, 325, 749
- Niemela, V. S., Marraco, H. G., & Cabanne, M. L. 1986, *PASP*, 98, 1133
- Parker, J. W., Garmany, C. D., Massey, P., & Walborn, N. R. 1992, *AJ*, 103, 1205
- Pols, O. R. & Marinus, M. 1994, *A&A*, 288, 475
- Preibisch, T., Balega, Y., Hofmann, K.-H., Weigelt, G., & Zinnecker, H. 1999, *NewA*, 4, 531
- Relaño, M., Peimbert, M., & Beckman, J. 2002, *ApJ*, 564, 704
- Robertson, J. W. 1974, *A&AS*, 15, 261
- Sanduleak, N. 1968, *AJ*, 73, 246
- Sanduleak, N. 1969, *Contrib. Cerro Tololo Inter-American Obs.*, No. 89
- Schaerer, D., Meynet, G., Maeder, A., & Schaller, G. 1993, *A&AS*, 98, 523
- Schmidt-Kaler, T. 1982, in *Landolt-Börnstein, Group VI, Vol 2b*, ed. K. Schaifers & H. H. Voigt (Springer-Verlag), 1
- Sebo, K. M. & Wood, P. R. 1994, *AJ*, 108, 932
- Slettebak, A. 1982, *ApJS*, 50, 55
- Smith, L. F., Shara, M. M., & Moffat, A. F. J. 1996, *MNRAS*, 281, 163
- Trundle, C. & Lennon, D. J. 2005, *A&A*, 434, 677
- Trundle, C., Lennon, D. J., Puls, J., & Dufton, P. L. 2004, *A&A*, 417, 217
- Vacca, W. D., Garmany, C. D., & Shull, M. J. 1996, *ApJ*, 460, 914
- Walborn, N. R. 1977, *ApJ*, 215, 53
- Walborn, N. R. 1980, *ApJS*, 44, 535
- Walborn, N. R. & Fitzpatrick, E. L. 1990, *PASP*, 102, 379
- Walborn, N. R. & Fitzpatrick, E. L. 2000, *PASP*, 112, 50
- Walborn, N. R., Howarth, I. D., Lennon, D. J., et al. 2002, *AJ*, 123, 2754
- Walborn, N. R., Lennon, D. J., Haser, S. M., Kudritzki, R.-P., & Voels, S. A. 1995, *PASP*, 107, 104
- Walborn, N. R., Lennon, D. J., Heap, S. R., et al. 2000, *PASP*, 112, 1243
- Walborn, N. R., Morrell, N. I., Howarth, I. D., et al. 2004, *ApJ*, 608, 1028
- Walborn, N. R. & Parker, J. W. 1992, *ApJ*, 399, L87
- Walker, M. F. 1961, *ApJ*, 133, 438
- Walker, M. F. 1987, *PASP*, 99, 179
- Weigelt, G., Balega, Y., Preibisch, T., et al. 1999, *A&A*, 347, L15
- Wellmann, P. 1952, *Zs. Astrophys.*, 30, 96
- Woolley, R. v. d. R. 1963, *Roy. Obs. Bull.*, 66, 263
- Zorec, J. & Briot, D. 1997, *A&A*, 318, 443

Table 4: NGC 346: Observational parameters of target stars. Cross-references to identifications by Sanduleak (1968, Sk), Azzopardi & Vignneau (1975, 1982, AzV), Niemela et al. (1986, NMC), Massey et al. (1989, MPG), Meyssonier & Azzopardi (1993, MA93), Keller et al. (1999, KWB), and Evans et al. (2004, 2dFS) are given in the final column. The radial velocities (v_r , in km s^{-1}) and radial distances to the centre of the cluster (r_d , in arcmin) are given for each star.

ID	EIS#	$\alpha(2000)$	$\delta(2000)$	r_d	V	$B - V$	Sp. Type	v_r	Comments
NGC 346-001†	SMC5_083194	00 59 31.94	-72 10 46.05	01.07	12.31	-0.19	O7 Iaf+	Binary	Sk 80, AzV 232, MPG 789, H α = broad em.
NGC 346-002	SMC5_082844	00 58 06.39	-72 07 05.47	06.62	13.22	-0.04	A2: Iab	-	FLAMES-UVES target
NGC 346-003	SMC5_082834	00 58 47.62	-72 13 31.01	03.58	13.56	0.62	G0:	-	FLAMES-UVES target; foreground
NGC 346-004	SMC5_082667	00 57 37.22	-72 13 09.12	08.06	13.69	-0.16	Be (B1:)	106: (8)	MA93#1021, AzV 191; H α = twin em.
NGC 346-005	SMC5_072019	00 57 21.47	-72 13 33.70	09.33	13.88	-0.02	A0 II	162 (5)	-
NGC 346-006	SMC5_000969	00 59 51.39	-72 14 49.23	04.76	14.02	0.15	F2:	-	FLAMES-UVES target
NGC 346-007	SMC5_079542	00 59 57.40	-72 10 33.53	01.59	14.07	-0.28	O4 V((f+))	Binary (SB1)	MPG 324, NMC 32
NGC 346-008	SMC5_081043	00 59 15.99	-72 04 44.46	06.06	14.20	-0.20	B1e	158 (6)	AzV 224; H α = twin em.
NGC 346-009	SMC5_028909	00 59 51.32	-72 11 28.57	02.64	14.36	-0.25	B0e	154 (7)	MPG 845, MA93#1167, H α = broad em.
NGC 346-010	SMC5_000836	00 59 20.70	-72 17 10.52	06.38	14.37	-0.22	O7 IIIIn(f)	208: (8)	AzV 226
NGC 346-011†	SMC5_075100	00 57 29.49	-72 16 00.40	09.80	14.39	-0.12	B9 II	160 (10)	-
NGC 346-012	SMC5_001361	00 58 14.46	-72 07 29.51	05.88	14.39	-0.23	B1 Ib	181 (13)	AzV 202
NGC 346-013	SMC5_072124	00 59 30.36	-72 09 09.59	01.89	14.46	0.06	B1:	Binary (SB2)	MPG 782
NGC 346-014	SMC5_026814	00 59 50.36	-72 13 57.16	04.01	14.58	0.01	A0 II	164 (5)	2dFS#1425
NGC 346-015	SMC5_022635	00 59 01.95	-72 18 52.91	08.17	14.62	-0.30	B1 V	Binary (SB2)	AzV 217, 2dFS#1357
NGC 346-016	SMC5_069563	00 59 36.19	-72 15 56.74	05.33	14.65	-0.23	B0.5 Vn	Binary (SB2)	2dFS#5100
NGC 346-017	SMC5_007202	00 58 11.94	-72 04 02.06	08.44	14.67	-0.22	Be (B1)	Binary	H α = twin em.
NGC 346-018	SMC5_038701	00 58 47.10	-72 13 01.57	03.25	14.78	-0.12	O9.5 IIIe	164 (3)	MPG 217, H α = em.
NGC 346-019	SMC5_031737	00 59 05.56	-72 08 02.38	02.92	14.82	-0.03	A0 II	162 (3)	-
NGC 346-020	SMC5_005500	00 57 46.46	-72 12 45.01	07.27	14.89	-0.22	B1 V+early-B	Binary (SB2)	2dFS#1259
NGC 346-021	SMC5_000965	00 59 19.58	-72 14 50.47	04.04	14.90	-0.18	B1 III	166 (11)	2dFS#5099
NGC 346-022	SMC5_005834	00 59 18.59	-72 11 09.89	00.37	14.91	-0.26	O9 V	156 (6)	MPG 682, NMC 40
NGC 346-023	SMC5_029130	00 58 41.86	-72 11 17.55	02.81	14.92	-0.07	B0.2: (Be-Fe)	161 (6)	MPG 178, MA93#1089, NMC 45, 2dFS#5097
NGC 346-024†	SMC5_078074	00 59 06.38	-72 07 44.97	03.18	14.92	-0.17	B2: shell (Be-Fe)	151 (5)	MA93#1118, KWB346#205, H α = twin
NGC 346-025	SMC5_056190	00 59 52.93	-72 10 49.07	02.67	14.95	-0.27	O9 V	Binary (SB1)	MPG 848
NGC 346-026†	SMC5_056277	00 58 14.10	-72 10 44.18	04.89	14.98	-0.14	B0 IV (Nstr)	222 (17)	MPG 12, 2dFS#1299
NGC 346-027	SMC5_032353	00 59 00.92	-72 07 18.16	03.73	15.00	-0.24	B0.5 V	166: (6)	-
NGC 346-028	SMC5_069506	00 59 31.77	-72 10 57.92	03.54	15.01	-0.26	OC6 Vz	178 (8)	MPG 113
NGC 346-029	SMC5_055586	00 59 14.53	-72 11 59.77	01.23	15.02	-0.19	B0 V	Binary (SB1)	MPG 637, NMC 50
NGC 346-030	SMC5_000991	00 58 55.97	-72 14 37.59	04.18	15.02	-0.21	B0 V	Binary	2dFS#5098
NGC 346-031	SMC5_034478	00 59 54.04	-72 04 31.28	06.86	15.02	-0.26	O8 Vz	159 (11)	-
NGC 346-032	SMC5_034263	00 59 24.81	-72 04 47.68	06.03	15.06	-0.26	B0.5 V	174 (11)	-
NGC 346-033†	SMC5_089286	00 59 11.62	-72 09 57.52	00.97	15.07	-0.25	O8 V	189: (3)	MPG 593
NGC 346-034	SMC5_029400	00 59 05.90	-72 10 50.28	00.93	15.08	-0.26	O8.5 V	Binary (SB1)	MPG 467, NMC 18
NGC 346-035	SMC5_001453	00 59 46.61	-72 05 32.45	05.70	15.09	-0.23	B1 V	Binary (SB2)	2dFS#1418
NGC 346-036†	SMC5_233890	00 59 23.33	-72 12 00.62	01.28	15.11	-0.07	B0.5 V (Be-Fe)	Binary?	MPG 729, MA93#1144
NGC 346-037	SMC5_032995	00 59 18.84	-72 06 29.27	04.31	15.18	-0.21	B3 III	153 (13)	-
NGC 346-038	SMC5_079698	00 58 51.33	-72 05 10.25	05.99	15.18	-0.24	B1 V	180 (7)	variable v_r ?
NGC 346-039	SMC5_075002	00 57 47.42	-72 16 40.44	09.08	15.19	-0.20	B0.7 V	156 (13)	2dFS#1262
NGC 346-040	SMC5_005698	00 58 23.59	-72 11 53.20	04.30	15.23	-0.16	B0.2 V	Binary (SB1)	MPG 61
NGC 346-041	SMC5_024945	00 57 44.32	-72 16 10.72	08.96	15.24	0.01	B2 (Be-Fe)	176 (9)	MA93#1030, H α = broad em.
NGC 346-042	SMC5_067681	00 59 36.26	-72 18 26.32	07.77	15.28	0.09	A7 II	122 (5)	-
NGC 346-043	SMC5_075935	00 58 13.95	-72 09 19.04	05.12	15.36	-0.23	B0 V	172 (16)	MPG 11
NGC 346-044	SMC5_081656	00 59 26.46	-72 13 11.78	02.48	15.38	-0.22	B1 II	146 (11)	MPG 753
NGC 346-045	SMC5_069093	00 58 24.19	-72 12 46.82	04.57	15.43	-0.20	B0.5 Vne	155 (5)	MPG 64, MA93#1070, H α = broad em.
NGC 346-046	SMC5_027160	00 59 31.84	-72 13 35.24	02.98	15.44	-0.28	O7 Vn	250: (8)	-
NGC 346-047	SMC5_006207	00 57 03.23	-72 09 15.03	10.43	15.45	-0.19	B2.5 III	137 (13)	2dFS#1189
NGC 346-048	SMC5_028019	00 58 47.50	-72 12 36.57	02.95	15.47	-0.21	Be (B3 shell)	165 (7)	MPG 222, KWB346#377, †, H α = twin
NGC 346-049	SMC5_026567	00 57 37.55	-72 14 17.54	08.44	15.50	-0.05	B8 II	144 (11)	-
NGC 346-050	SMC5_075959	00 58 55.22	-72 09 06.57	02.43	15.50	-0.30	O8 Vn	160 (5)	MPG 299
NGC 346-051	SMC5_038979	00 59 08.68	-72 10 14.08	00.91	15.51	-0.26	O7 Vz	169 (9)	MPG 523, NMC 38
NGC 346-052	SMC5_000921	00 58 07.49	-72 15 47.98	07.36	15.52	-0.23	B1.5 V	Binary (SB1)	-
NGC 346-053	SMC5_004887	00 57 57.68	-72 16 02.24	08.07	15.52	-0.25	B0.5 V	Binary (SB1)	-
NGC 346-054	SMC5_038674	00 58 56.51	-72 13 13.43	02.93	15.59	-0.15	B1 V	164 (8)	MPG 309
NGC 346-055	SMC5_001131	00 58 27.59	-72 11 54.55	04.01	15.59	-0.15	B0.5 V	176 (6)	MPG 84, MA93#1072
NGC 346-056	SMC5_079574	00 58 56.12	-72 09 33.84	02.08	15.59	-0.26	B0 V	178 (11)	MPG 310, NMC 48
NGC 346-057	SMC5_032947	00 59 52.69	-72 06 29.50	05.06	15.62	-0.23	B2.5 III	143 (9)	MA93#1169, KWB346#526, †, str. nebular lines
NGC 346-058	SMC5_001067	00 59 31.53	-72 13 06.46	02.53	15.63	-0.22	B0.5 V	Binary (SB1)	MPG 787
NGC 346-059	SMC5_076160	00 58 04.83	-72 07 17.70	06.60	15.64	0.09	A5 II	188 (5)	-
NGC 346-060	SMC5_033513	00 59 19.28	-72 05 47.80	05.00	15.68	-0.13	B0.5e (shell)	142 (5)	MA93#1140, KWB346#236, H α = twin
NGC 346-061	SMC5_082792	00 57 57.82	-72 07 55.43	06.78	15.70	-0.21	B1-2 (Be-Fe)	152: (4)	KWB346#122, 2dFS#1277, †, H α = broad em.
NGC 346-062	SMC5_039483	00 59 56.61	-72 05 08.50	06.38	15.70	-0.24	B0.2 V	136 (15)	-
NGC 346-063	SMC5_005036	00 59 44.87	-72 15 11.43	04.85	15.72	-0.03	A0 II	118 (5)	2dFS#1413
NGC 346-064	SMC5_006226	00 57 55.47	-72 09 05.86	06.54	15.72	-0.13	B1-2 (Be-Fe)	162 (6)	MA93#1043, KWB346#289, H α = broad em.
NGC 346-065	SMC5_083005	00 58 47.53	-72 09 02.70	02.92	15.73	-0.15	B3 (Be-Fe)	132 (8)	MPG 228, KWB346#379, †, H α = twin
NGC 346-066	SMC5_001152	00 58 45.98	-72 11 36.78	02.58	15.75	-0.25	O9.5 V	163 (5)	MPG 213; variable v_r ?
NGC 346-067	SMC5_001335	00 57 50.38	-72 07 56.04	07.29	15.76	-0.04	B1-2 (Be-Fe)	172: (8)	MA93#1038, H α = twin
NGC 346-068	SMC5_076404	00 59 04.14	-72 04 48.72	06.08	15.77	-0.17	B0 V (Be-Fe)	Binary	H α = broad em.
NGC 346-069	SMC5_005388	00 57 07.29	-72 13 19.31	10.31	15.80	-0.10	B1-2 (Be-Fe)	138: (6)	MA93#981, H α = broad em.
NGC 346-070	SMC5_026922	00 59 15.49	-72 13 52.21	03.08	15.82	-0.22	B0.5 V	165: (13)	-
NGC 346-071	SMC5_052484	01 00 04.21	-72 16 47.56	06.96	15.84	-0.07	A0 II	178 (2)	-
NGC 346-072†	SMC5_055979	00 58 22.65	-72 11 17.86	04.26	15.84	-0.10	B1-2 (Be-Fe)	153 (6)	MPG 54, MWB143, H α = broad em.
NGC 346-073	SMC5_025100	01 00 05.24	-72 15 55.54	06.27	15.84	-0.17	B1-2 (Be-Fe)	143 (5)	MA93#1183, H α = broad em.
NGC 346-074	SMC5_000748	00 58 55.81	-72 18 41.29	08.07	15.85	-0.22	B3 III	142 (12)	-
NGC 346-075	SMC5_006828	00 59 25.96	-72 06 01.45	04.81	15.85	-0.26	B1 V	Binary (SB1)	2dFS#1389
NGC 346-076	SMC5_055468	00 59 12.12	-72 12 11.69	01.47	15.87	0.05	B2 (Be-Fe)	172: (4)	MPG 596, KWB346#445, †, H α = broad em.
NGC 346-077	SMC5_030292	00 58 48.97	-72 09 51.92	02.41	15.88	-0.18	O9 V	165 (6)	MPG 238, NMC 39
NGC 346-078	SMC5_026141	00 58 22.07	-72 14 45.69	05.83	15.88	-0.21	B2 III	Binary	-

continued on next page

Table 4: *continued*

ID	EIS#	$\alpha(2000)$	$\delta(2000)$	r_d	V	$B - V$	Sp. Type	v_r	Comments
NGC 346-079	SMC5_029544	00 59 03.05	-72 10 44.07	$\phi 1.15$	15.88	-0.23	B0.5 Vn	168 (4)	MPG 400
NGC 346-080	SMC5_029906	00 58 49.61	-72 10 19.52	$\phi 2.22$	15.89	-0.11	B1 V	160: (6)	MPG 243, NMC 47, H α = broad em.,neb?
NGC 346-081	SMC5_027589	00 58 00.38	-72 13 07.86	$\phi 6.38$	15.91	-0.20	B2 III _n	148 (10)	
NGC 346-082	SMC5_026587	00 58 08.32	-72 14 16.49	$\phi 6.36$	15.91	-0.21	B2 III	Binary (SB1)	
NGC 346-083	SMC5_005921	00 59 28.07	-72 10 42.23	$\phi 0.78$	15.91	-0.24	B1 V	172: (5)	MPG 767
NGC 346-084	SMC5_001425	00 58 13.04	-72 06 02.88	$\phi 6.88$	15.92	-0.23	B1 V	147 (8)	2dFS#1296
NGC 346-085	SMC5_030007	00 57 37.95	-72 10 13.78	$\phi 7.68$	15.93	-0.22	B2 III	Binary (SB1)	
NGC 346-086	SMC5_056528	00 59 01.92	-72 10 21.33	$\phi 1.31$	15.94	-0.25	B0.2 V	Binary (SB1)	MPG 371
NGC 346-087	SMC5_052697	00 59 21.91	-72 16 27.37	$\phi 5.66$	15.95	0.00	A0 II	115 (6)	
NGC 346-088	SMC5_024131	00 59 07.82	-72 17 06.01	$\phi 6.35$	15.95	-0.22	B1 V	174 (11)	
NGC 346-089	SMC5_023010	00 59 10.87	-72 18 27.92	$\phi 7.68$	15.96	-0.17	B1-2 (Be-Fe)	185 (6)	MA93#1123, H α = twin em.
NGC 346-090	SMC5_026342	00 58 25.73	-72 14 33.19	$\phi 5.48$	15.96	-0.18	O9.5 V	172 (7)	
NGC 346-091	SMC5_022851	00 58 29.64	-72 18 40.58	$\phi 8.70$	15.98	-0.18	B1e	Binary (SB1)	MA93#1075, H α =broad em.
NGC 346-092	SMC5_032179	00 59 42.36	-72 07 27.12	$\phi 3.83$	16.00	-0.27	B1 Vn	157: (6)	
NGC 346-093	SMC5_069704	00 58 55.60	-72 10 07.19	$\phi 1.84$	16.01	-0.19	B0 V	157 (6)	MPG 304
NGC 346-094	SMC5_006635	00 59 57.22	-72 07 00.28	$\phi 4.84$	16.01	-0.31	B0.7 V	138 (13)	
NGC 346-095	SMC5_004916	00 57 40.34	-72 15 51.42	$\phi 9.02$	16.04	-0.05	B1-2 (Be-Fe)	162: (6)	MA93#1027, H α =broad em.
NGC 346-096	SMC5_033169	00 57 28.87	-72 06 19.25	$\phi 9.47$	16.04	-0.08	B1-2 (Be-Fe)	185: (6)	MA93#1009, H α =broad em.
NGC 346-097	SMC5_005824	00 59 08.53	-72 11 12.56	$\phi 0.83$	16.06	-0.07	O9 V	159 (8)	MPG 519, NMC 6
NGC 346-098	SMC5_005427	00 59 11.01	-72 13 04.04	$\phi 2.33$	16.09	-0.22	B1.5 V	158 (9)	MPG 568
NGC 346-099	SMC5_060385	00 58 02.32	-72 03 12.37	$\phi 9.55$	16.10	-0.18	B3 III	157 (10)	
NGC 346-100	SMC5_007269	00 59 20.66	-72 03 38.00	$\phi 7.17$	16.10	-0.24	B1.5 V	152 (6)	
NGC 346-101	SMC5_056629	00 57 59.80	-72 10 11.61	$\phi 6.01$	16.15	-0.23	B1 V	184 (13)	
NGC 346-102	SMC5_058504	00 58 12.30	-72 06 52.07	$\phi 6.38$	16.16	-0.17	B3 III	144 (11)	
NGC 346-103	SMC5_007370	00 59 20.82	-72 02 58.58	$\phi 7.83$	16.16	-0.30	B0.5 V	137 (16)	
NGC 346-104†	SMC5_089334	00 59 13.76	-72 09 27.36	$\phi 1.38$	16.16	-0.34	B0 V	Binary (SB1)	MPG 628,MA93#1129, H α = str. em.
NGC 346-105	SMC5_069135	00 58 28.48	-72 12 34.27	$\phi 4.18$	16.19	-0.11	B2 III	Binary	MPG 88
NGC 346-106	SMC5_004992	00 57 52.24	-72 15 28.18	$\phi 8.05$	16.19	-0.17	B1 V	Binary	
NGC 346-107	SMC5_001206	00 59 10.37	-72 10 28.45	$\phi 0.67$	16.20	-0.27	O9.5 V	156 (7)	MPG 559, NMC 22
NGC 346-108	SMC5_006368	00 59 58.11	-72 08 21.80	$\phi 3.92$	16.21	-0.28	B1.5 V	160 (6)	
NGC 346-109	SMC5_089444	00 59 19.39	-72 04 29.11	$\phi 6.32$	16.21	-0.29	B1.5 V	169: (6)	
NGC 346-110	SMC5_005120	00 58 11.49	-72 14 42.70	$\phi 6.42$	16.22	-0.15	B1-2 (Be-Fe)	Binary	KWB346#313, H α = twin em.
NGC 346-111	SMC5_082079	00 59 00.16	-72 10 46.66	$\phi 1.37$	16.24	-0.24	B0.5 V	163 (5)	MPG 344
NGC 346-112	SMC5_005637	00 58 58.54	-72 12 06.72	$\phi 1.98$	16.24	-0.24	O9.5 V	162 (5)	MPG 327
NGC 346-113	SMC5_006076	00 58 11.22	-72 09 59.08	$\phi 5.17$	16.27	-0.27	B0.5 V	177: (13)	variable v_r ?
NGC 346-114	SMC5_031881	01 00 02.66	-72 07 48.68	$\phi 4.54$	16.28	-0.30	B1 Vn	174: (6)	
NGC 346-115†	SMC5_075795	00 59 04.63	-72 10 31.16	$\phi 1.06$	16.30	-0.28	B0.2 V	182 (7)	MPG 443
NGC 346-116	SMC5_076289	01 00 03.23	-72 06 03.65	$\phi 5.87$	16.30	-0.30	B1 V	154 (13)	

†: Further notes on individual stars:

NGC 346-001: saturated in images, photometry is from MPG

NGC 346-011: member of Lindsay 56/LHA 115-S26

NGC 346-024: is also KWB346#72, blended with SMC5_078073

NGC 346-026: faint companions in WFI images

NGC 346-033: blended in images with SMC5_080234

NGC 346-036: bad column in V image, photometry is from MPG

NGC 346-048: is also MA93#1101

NGC 346-057: blended in images with SMC5_032946

NGC 346-061: is also MA93#1048

NGC 346-065: is also MA93#1100

NGC 346-072: correlated with MA93#1067, which is resolved into two bright components in WFI image

NGC 346-076: is also MA93#1126

NGC 346-104: part blended with SMC5_082742/MPG 635

NGC 346-115: part blended with SMC5_246984/MPG 426

Table 5: NGC 330: Observational parameters of target stars. Cross-references to identifications given by Sanduleak (1968, Sk), Arrp (1959), Robertson (1974, R74), Azzopardi & Vigneau (1975, 1982, AzV), Meyssonnier & Azzopardi (1993, MA93), Keller et al. (1999, KWB) and Evans et al. (2004, 2dFS) are given in the final column. The radial velocities (v_r , in km s^{-1}) and radial distances to the centre of the cluster (r_d , in arcmin) are given for each star.

ID	EIS#	$\alpha(2000)$	$\delta(2000)$	r_d	V	$B - V$	Sp. Type	v_r	Comments
NGC 330-001	SMC5_078698	00 55 48.34	-72 30 52.90	03.85	12.99	0.03	B9-A0 Iab	—	FLAMES-UVES target
NGC 330-002	SMC5_082820	00 56 24.85	-72 27 41.79	00.46	13.03	-0.04	B3 Ib	154 (20)	R74-A02
NGC 330-003	SMC5_081785	00 56 55.29	-72 24 20.55	04.41	13.17	0.00	B2 Ib	147 (17)	Sk 65, AzV 180, 2dFS#1183; $H\alpha$ = infilled abs.
NGC 330-004	SMC5_082763	00 56 20.80	-72 28 33.98	00.79	13.33	-0.07	B2.5 Ib	157 (16)	R74-B37, 2dFS#5090; $H\alpha$ = infilled abs.
NGC 330-005	SMC5_082862	00 55 04.93	-72 29 22.87	05.79	13.35	-0.06	B5 Ib	150 (15)	
NGC 330-006	SMC5_082471	00 56 38.18	-72 18 37.72	09.27	13.41	0.02	A3: II	—	FLAMES-UVES target
NGC 330-007	SMC5_082854	00 56 58.26	-72 31 17.34	04.59	13.48	0.23	A7-F0 II	—	FLAMES-UVES target
NGC 330-008	SMC5_082532	00 56 09.63	-72 32 28.56	04.74	13.71	0.23	A7-F0 II	—	FLAMES-UVES target
NGC 330-009	SMC5_082706	00 53 53.75	-72 26 49.99	10.97	13.72	-0.06	B5 Ib	139 (11)	
NGC 330-010	SMC5_082798	00 54 55.21	-72 33 26.49	08.46	13.89	-0.03	B5 Ib	142 (10)	
NGC 330-011	SMC5_051901	00 56 56.75	-72 17 44.71	10.44	13.91	-0.02	B9 Ib	156 (6)	AzV 181
NGC 330-012	SMC5_015870	00 56 07.95	-72 26 03.74	01.91	13.92	-0.01	A0 Ib	128 (6)	Arp 211
NGC 330-013	SMC5_001959	00 57 26.97	-72 33 13.30	07.48	14.00	-0.13	O8.5 II-III ((f))	176 (11)	AzV 186, 2dFS#1230
NGC 330-014	SMC5_081774	00 56 38.79	-72 25 13.75	02.97	14.07	-0.12	B1.5 Ib	159 (15)	AzV 176
NGC 330-015	SMC5_003863	00 55 21.62	-72 21 50.23	07.35	14.27	0.15	A7-F0 II	—	AzV 167; FLAMES-UVES target
NGC 330-016	SMC5_073986	00 55 21.48	-72 23 38.01	05.99	14.28	-0.14	B5: II	130 (12)	contaminated by arcs
NGC 330-017	SMC5_064339	00 56 47.98	-72 28 46.86	02.41	14.35	-0.11	B2 II	157 (15)	AzV 178, 2dFS#1171
NGC 330-018	SMC5_078858	00 56 09.41	-72 27 58.71	00.73	14.37	-0.13	B3 II	153 (11)	R74-B30
NGC 330-019	SMC5_037327	00 55 52.85	-72 26 31.42	02.33	14.38	-0.03	B9 Ib	127 (8)	
NGC 330-020	SMC5_002300	00 57 28.08	-72 31 03.34	06.16	14.43	-0.03	B3 II	158 (14)	2dFS#1232
NGC 330-021	SMC5_003855	00 57 37.34	-72 21 53.94	08.35	14.45	-0.25	B0.2 III	173 (10)	AzV 192, 2dFS#1242
NGC 330-022	SMC5_002377	00 55 15.68	-72 30 33.73	05.51	14.56	-0.13	B3 II	147 (16)	2dFS#1062
NGC 330-023	SMC5_190576	00 56 44.31	-72 29 06.33	02.33	14.56	-0.12	O9 V-IIIe	159: (3)	KWB330#111, $H\alpha$ = strong em.
NGC 330-024	SMC5_065615	00 54 58.57	-72 25 09.71	06.59	14.72	-0.06	B5 Ib	161 (11)	2dFS#1034
NGC 330-025	SMC5_037578	00 57 23.98	-72 23 56.49	06.24	14.81	-0.11	B1.5e	110: (7)	2dFS#1224, $H\alpha$ = twin
NGC 330-026	SMC5_019099	00 57 23.40	-72 22 45.68	07.00	14.82	-0.15	B2.5 II	152 (11)	
NGC 330-027	SMC5_003910	00 56 18.27	-72 21 33.39	06.23	14.86	-0.16	B1 V	170 (11)	
NGC 330-028	SMC5_002054	00 57 06.05	-72 32 39.25	06.03	14.94	-0.11	B1 V	172 (9)	2dFS#1195
NGC 330-029	SMC5_000205	00 57 00.18	-72 30 09.78	03.92	14.97	-0.09	B0.2 V (Be-Fe)	Binary	MA93#973, KWB330#104, \dagger , $H\alpha$ = em.
NGC 330-030	SMC5_020391	00 56 23.58	-72 21 23.64	06.40	14.99	-0.26	B0.5 V	Binary	
NGC 330-031	SMC5_002476	00 56 13.84	-72 30 00.77	02.26	15.00	-0.04	B0.5 V (Be-Fe)	146 (4)	2dFS#5088, $H\alpha$ = em.
NGC 330-032	SMC5_076906	00 57 38.56	-72 30 38.67	06.65	15.07	-0.10	B0.5 V	162 (19)	
NGC 330-033	SMC5_079846	00 57 10.52	-72 30 04.17	04.52	15.08	-0.11	B1.5 V	177: (9)	2dFS#5094, variable v_r ?, contaminated by arcs
NGC 330-034	SMC5_000183	00 54 40.74	-72 30 28.56	07.86	15.09	-0.09	B1-2e	121: (5)	MA93#794
NGC 330-035	SMC5_009426	00 57 23.92	-72 32 37.52	06.89	15.09	-0.07	B3 II	143 (12)	
NGC 330-036	SMC5_044567	00 56 10.66	-72 28 10.25	00.72	15.10	-0.16	B2 II	156 (16)	R74-B32
NGC 330-037	SMC5_004102	00 55 09.80	-72 20 24.65	09.02	15.12	-0.02	A2 II	145 (5)	2dFS#1058
NGC 330-038	SMC5_014400	00 57 15.31	-72 27 33.94	04.26	15.21	-0.19	B1 V	133: (9)	2dFS#1206
NGC 330-039	SMC5_003405	00 55 55.67	-72 24 32.80	03.68	15.26	-0.22	B0 V	173: (9)	2dFS#1109
NGC 330-040	SMC5_007692	00 55 03.41	-72 34 12.96	08.58	15.29	-0.05	B2 III	152 (7)	2dFS#1041
NGC 330-041	SMC5_077354	00 57 37.17	-72 23 55.97	07.05	15.38	-0.24	B0 V	184 (10)	2dFS#1241
NGC 330-042	SMC5_016204	00 56 27.09	-72 25 42.59	02.17	15.41	-0.16	B2 II	130 (12)	
NGC 330-043	SMC5_046989	00 56 27.11	-72 25 04.74	02.78	15.47	-0.19	B0 V	161: (6)	
NGC 330-044	SMC5_037013	00 55 13.61	-72 29 13.69	05.12	15.50	-0.02	B1-2 (Be-Fe)	158: (5)	MA93#824
NGC 330-045	SMC5_003118	00 56 05.59	-72 26 21.48	01.74	15.54	-0.15	B3 III	159 (3)	2dFS#5087
NGC 330-046	SMC5_088493	00 58 12.39	-72 26 12.09	08.70	15.56	-0.14	O9.5 V	177 (6)	2dFS#1293
NGC 330-047	SMC5_021183	00 57 03.45	-72 20 35.41	07.94	15.61	-0.28	B1 V	176 (13)	2dFS#1190, variable v_r ?
NGC 330-048	SMC5_042483	00 55 35.03	-72 30 51.53	04.51	15.62	-0.19	B0.5 V	181 (6)	
NGC 330-049	SMC5_086635	00 55 59.58	-72 23 31.30	04.50	15.63	-0.27	O9 V	158 (8)	
NGC 330-050	SMC5_004159	00 56 56.44	-72 20 07.40	08.17	15.66	-0.18	B3e	113 (7)	MA93#969, $H\alpha$ = twin
NGC 330-051	SMC5_082766	00 57 57.69	-72 27 10.54	07.47	15.66	-0.16	B1.5 V	174 (5)	2dFS#1276
NGC 330-052	SMC5_000744	00 56 31.00	-72 18 52.99	08.95	15.69	-0.26	O8.5 Vn	166: (7)	2dFS#1152
NGC 330-053†	SMC5_013120	00 57 58.81	-72 28 50.68	07.61	15.69	-0.12	B0.5 V	167 (10)	variable v_r ?
NGC 330-054	SMC5_037029	00 55 28.20	-72 29 06.50	04.03	15.70	-0.08	B2 (Be-Fe)	127: (6)	MA93#851, $H\alpha$ = em.
NGC 330-055	SMC5_012510	00 56 49.24	-72 29 28.96	02.85	15.72	-0.11	B0.5 V	174: (7)	variable v_r ?
NGC 330-056	SMC5_002447	00 55 23.37	-72 30 09.56	04.80	15.76	-0.19	B2 III	122: (9)	
NGC 330-057	SMC5_009833	00 54 54.63	-72 32 09.58	07.70	15.82	-0.17	B0.5 V	124: (4)	
NGC 330-058	SMC5_036895	00 54 58.54	-72 30 22.38	06.58	15.84	-0.11	B3:	112: (2)	
NGC 330-059	SMC5_002498	00 57 52.13	-72 29 51.87	07.33	15.85	-0.08	B3 III	151: (11)	
NGC 330-060	SMC5_011393	00 55 59.43	-72 30 34.33	03.14	15.86	-0.06	B2.5 (Be-Fe)	156: (7)	MA93#890, $H\alpha$ = em.
NGC 330-061	SMC5_004133	00 56 00.52	-72 20 15.94	07.65	15.88	-0.10	A0 II	131 (3)	2dFS#1118
NGC 330-062	SMC5_045835	00 56 18.05	-72 26 35.82	01.19	15.90	-0.10	B3e	156: (6)	$H\alpha$ = twin
NGC 330-063	SMC5_080598	00 56 06.81	-72 30 28.62	02.84	15.90	-0.06	B1-3	121: (9)	
NGC 330-064	SMC5_061057	00 55 45.87	-72 33 13.06	05.97	15.96	-0.09	B3:e	135 (4)	
NGC 330-065	SMC5_002751	00 56 14.27	-72 28 30.13	00.79	15.99	-0.04	B1-3 (Be-Fe)	158: (8)	R74-B34, KWB330#239, \dagger , $H\alpha$ = em.
NGC 330-066	SMC5_010645	00 55 55.96	-72 31 19.82	03.94	15.99	-0.10	B3 III	152 (8)	
NGC 330-067	SMC5_079924	00 55 34.83	-72 27 18.75	03.35	16.00	-0.17	B2.5 III	141 (8)	
NGC 330-068	SMC5_009989	00 55 35.52	-72 32 00.30	05.33	16.02	-0.06	B1.5 (Be-Fe)	133 (9)	MA93#860, $H\alpha$ = twin
NGC 330-069	SMC5_043375	00 56 48.62	-72 29 40.11	02.93	16.02	-0.05	B3 III	160: (7)	
NGC 330-070	SMC5_077231	00 57 02.19	-72 25 55.33	03.76	16.02	-0.05	B0.5e	128 (4)	$H\alpha$ = twin
NGC 330-071	SMC5_014767	00 56 59.92	-72 27 04.66	03.18	16.03	-0.09	B3 III	134 (10)	
NGC 330-072	SMC5_017978	00 56 09.16	-72 23 55.23	03.93	16.03	-0.20	B0.5 V	136: (6)	
NGC 330-073	SMC5_047763	00 55 42.62	-72 23 58.22	04.69	16.04	-0.08	B8 Ib	58 (6)	KWB330#522, \dagger , $H\alpha$ = em., variable v_r ?
NGC 330-074	SMC5_002782	00 54 41.61	-72 28 15.74	07.34	16.09	-0.24	B0 V	156 (6)	
NGC 330-075	SMC5_004413	00 55 52.41	-72 18 45.05	09.25	16.10	-0.17	B8 II	131: (3)	
NGC 330-076	SMC5_014864	00 56 33.11	-72 27 04.99	01.29	16.12	-0.05	B3 (Be-Fe)	126: (10)	R74-B09, KWB330#419, \dagger , $H\alpha$ = em.
NGC 330-077	SMC5_000166	00 55 43.22	-72 30 49.00	04.05	16.13	-0.01	B0-3 (Be-Fe)	—	\dagger , low S/N, strongly contaminated by arcs
NGC 330-078	SMC5_003498	00 55 11.95	-72 23 54.90	06.35	16.15	-0.03	A0: III	112 (2)	

continued on next page

Table 5: *continued*

ID	EIS#	$\alpha(2000)$	$\delta(2000)$	r_d	V	$B - V$	Sp. Type	v_r	Comments
NGC 330-079	SMC5_037369	00 55 52.41	-72 26 11.32	\varnothing 2.55	16.16	-0.13	B3 III	155 (5)	variable v_r ?
NGC 330-080	SMC5_037034	00 57 35.30	-72 29 04.90	\varnothing 5.91	16.17	-0.07	B1-3	141: (5)	MA93#1019
NGC 330-081	SMC5_044096	00 56 02.28	-72 28 44.96	\varnothing 1.57	16.17	-0.16	B1-3	130: (8)	
NGC 330-082	SMC5_044447	00 57 24.60	-72 28 17.06	\varnothing 4.98	16.18	-0.07	B1-3	141: (8)	contaminated by arcs
NGC 330-083	SMC5_087520	00 57 04.56	-72 22 53.62	\varnothing 5.99	16.19	-0.13	B3 III	140 (9)	
NGC 330-084	SMC5_044140	00 55 36.33	-72 28 40.84	\varnothing 3.32	16.20	-0.08	B3 III-V	Binary (SB1)	
NGC 330-085	SMC5_073581	00 56 26.60	-72 26 23.02	\varnothing 1.52	16.22	-0.12	B3:e	110: (3)	H α = twin
NGC 330-086	SMC5_012975	00 56 33.74	-72 29 01.55	\varnothing 1.67	16.25	-0.15	B2.5 III	128: (9)	R74-B01
NGC 330-087	SMC5_000135	00 55 43.50	-72 31 32.61	\varnothing 4.60	16.26	-0.12	Be-Fe	—	MA93#869, H α = em.
NGC 330-088	SMC5_009618	00 55 56.53	-72 32 25.98	\varnothing 4.94	16.30	-0.14	B1-3	—	
NGC 330-089	SMC5_002393	00 55 37.99	-72 30 27.19	\varnothing 4.07	16.32	-0.17	B1-5	154: (4)	contaminated by arcs
NGC 330-090	SMC5_073266	00 55 44.03	-72 28 10.44	\varnothing 2.65	16.34	-0.15	B3 III	117: (5)	
NGC 330-091	SMC5_080521	00 57 05.74	-72 33 41.81	\varnothing 6.89	16.34	-0.13	B0e	162 (7)	H α = twin+abs.
NGC 330-092	SMC5_002411	00 57 48.75	-72 30 19.28	\varnothing 7.23	16.35	-0.03	B3:	—	
NGC 330-093	SMC5_036967	00 55 40.11	-72 29 44.78	\varnothing 3.51	16.36	-0.14	Be-Fe	—	MA93#863, KWB330#528, H α = twin
NGC 330-094	SMC5_082714	00 55 33.33	-72 23 57.34	\varnothing 5.14	16.36	-0.21	B1-5	179: (2)	contaminated by arcs
NGC 330-095	SMC5_014467	00 56 15.39	-72 27 29.32	\varnothing 0.39	16.38	-0.15	B3 III	155 (10)	
NGC 330-096	SMC5_014644	00 54 39.14	-72 27 16.74	\varnothing 7.52	16.38	-0.08	B1-3 (Be-Fe)	—	MA93#782, H α = em.
NGC 330-097	SMC5_002965	00 56 17.13	-72 27 17.95	\varnothing 0.50	16.40	-0.19	B1 V	148: (7)	
NGC 330-098	SMC5_065934	00 56 07.74	-72 24 18.13	\varnothing 3.58	16.40	-0.24	B0.2: V	175: (2)	contaminated by arcs
NGC 330-099	SMC5_044674	00 55 01.81	-72 28 01.35	\varnothing 5.80	16.41	-0.18	B2-3	—	
NGC 330-100	SMC5_002442	00 56 54.25	-72 30 12.22	\varnothing 3.60	16.43	0.00	Be (B0-3)	—	H α = twin
NGC 330-101	SMC5_002817	00 56 35.34	-72 28 06.57	\varnothing 1.29	16.44	-0.14	B2.5 III	154 (8)	
NGC 330-102	SMC5_014776	00 57 12.14	-72 27 10.37	\varnothing 4.06	16.46	-0.16	B2-3 III	162: (5)	
NGC 330-103	SMC5_002256	00 56 52.31	-72 31 18.50	\varnothing 4.33	16.47	-0.07	B1-3	—	contaminated by arcs
NGC 330-104	SMC5_048561	00 55 01.81	-72 22 49.67	\varnothing 7.63	16.50	-0.30	B0: V	129: (4)	2dFS#1037
NGC 330-105	SMC5_020588	00 57 05.64	-72 21 11.89	\varnothing 7.47	16.53	-0.17	B1-3	—	
NGC 330-106	SMC5_011915	00 56 35.13	-72 29 58.90	\varnothing 2.52	16.54	-0.15	B1-2	135 (12)	
NGC 330-107	SMC5_014046	00 55 57.78	-72 27 51.05	\varnothing 1.58	16.56	-0.12	B3: III-V	138 (5)	
NGC 330-108	SMC5_015203	00 55 14.50	-72 26 43.73	\varnothing 4.96	16.56	-0.13	B5 III	126: (2)	
NGC 330-109	SMC5_065064	00 56 24.94	-72 26 48.43	\varnothing 1.08	16.56	-0.17	B3 III	144: (4)	
NGC 330-110	SMC5_037341	00 56 20.67	-72 26 25.49	\varnothing 1.37	16.57	-0.19	B2 III	160: (6)	
NGC 330-111	SMC5_013331	00 56 17.70	-72 28 37.71	\varnothing 0.85	16.58	-0.17	B1-3	—	
NGC 330-112	SMC5_048045	00 55 56.33	-72 23 33.34	\varnothing 4.56	16.59	-0.11	B1-3 (Be-Fe)	—	MA93#886, KWB330#509, H α = em.
NGC 330-113	SMC5_015068	00 55 48.73	-72 26 51.42	\varnothing 2.45	16.61	-0.14	B1-3	—	
NGC 330-114	SMC5_078349	00 56 57.01	-72 25 31.71	\varnothing 3.66	16.62	-0.14	B2 III	157 (11)	
NGC 330-115	SMC5_061511	00 55 15.38	-72 24 23.49	\varnothing 5.86	16.65	-0.26	B1-3	Binary	
NGC 330-116	SMC5_045013	00 55 26.53	-72 27 33.66	\varnothing 3.94	16.66	-0.19	B3 III	133 (6)	
NGC 330-117	SMC5_049053	00 56 39.75	-72 22 06.43	\varnothing 5.89	16.67	-0.21	B1-3	120: (6)	
NGC 330-118	SMC5_037899	00 54 47.70	-72 20 51.51	\varnothing 9.75	16.69	-0.26	B1-2	170 (4)	2dFS#1013
NGC 330-119	SMC5_191730	00 56 45.39	-72 27 55.47	\varnothing 2.01	16.71	-0.22	B1-3	—	
NGC 330-120	SMC5_191173	00 56 42.59	-72 27 27.78	\varnothing 1.82	16.89	-0.42	B3: III-V	147: (5)	
NGC 330-121	SMC5_081980	00 56 22.57	-72 28 35.68	\varnothing 0.86	12.62	0.20	A5 II	154 (5)	R74-B38; UVES target
NGC 330-122	SMC5_015195	00 56 18.56	-72 26 45.21	\varnothing 1.03	14.00	0.04	A2 II	138 (5)	R74-B16; UVES target
NGC 330-123	SMC5_037226	00 56 03.92	-72 27 13.01	\varnothing 1.26	15.79	-0.22	O9.5 V	177 (11)	R74-B18; UVES target
NGC 330-124	SMC5_013293	00 56 06.81	-72 28 35.08	\varnothing 1.21	15.83	-0.20	B0.2 V	155 (12)	R74-B28; UVES target
NGC 330-125	SMC5_003014	00 56 20.18	-72 27 02.02	\varnothing 0.76	15.89	-0.17	B2 III	151 (8)	R74-B13; UVES target

†: Further notes on individual stars:

NGC 330-029: is also 2dFS#5093

NGC 330-053: 2dFS#1279 is likely a blend of 330-053 & SMC5_064320

NGC 330-065: is also MA93#920

NGC 330-073: is also 2dFS#1087

NGC 330-076: is also MA93#948

NGC 330-077: is also MA93#868

Table 6: N11: Observational parameters of target stars. The cross-references in the final column are to Sanduleak (1969, Sk) and Parker et al. (1992, P) The photometry for stars flagged with an asterisk was taken from Parker et al. (1992). Classifications for N11-031 and N11-060 were taken from Walborn et al. (2002) and Walborn et al. (2004) respectively.

ID	$\alpha(2000)$	$\delta(2000)$	V	$B - V$	Sp. Type	v_r	Comments
N11-001	04 57 08.85	-66 23 25.1	11.35*	0.06	B2 Ia	299 (12)	Sk-66° 36, P3252; UVES spectrum, H α = P Cyg em.
N11-002	04 56 23.51	-66 29 51.7	11.90*	0.37	B3 Ia	295 (12)	Sk-66° 27, P1062; UVES spectrum, H α = P Cyg em.
N11-003	04 56 50.59	-66 24 34.9	12.47*	-0.02	B1 Ia	287 (12)	P3157; UVES spectrum, H α = broad em.
N11-004	04 55 29.42	-66 23 12.0	12.56	-0.06	O9.7 Ib	304 (15)	Sk-66° 16
N11-005	04 57 04.10	-66 29 10.1	12.62	0.03	B1 Ia	Binary	Sk-66° 34, H α = em.
N11-006	04 56 51.45	-66 28 06.4	12.66	0.51	F8:	-	FLAMES-UVES target, foreground
N11-007	04 56 17.29	-66 31 03.6	12.74	-0.03	O8 Ib (f)	302 (14)	Sk-66° 25, variable v_r or wind var.?
N11-008	04 55 22.35	-66 28 18.9	12.77	-0.01	B0.5 Ia	288 (14)	Sk-66° 15
N11-009	04 57 17.68	-66 26 31.5	12.80	0.06	B3 Iab	288 (15)	
N11-010	04 56 40.94	-66 27 40.1	12.89	-0.14	O9.5 III + B1-2:	Binary (SB2)	P1310
N11-011	04 55 55.50	-66 28 20.3	12.89	-0.08	OC9.5 II	Binary (SB1)	Sk-66° 17
N11-012	04 56 51.15	-66 31 48.3	12.90	0.02	B1 Ia	295 (11)	variable v_r ?
N11-013	04 57 00.86	-66 24 24.8	12.93	-0.07	O8 V	Binary (SB2)	P3223
N11-014	04 56 48.02	-66 20 09.8	12.98	-0.02	B2 Iab	298 (13)	Sk-66° 30
N11-015	04 57 22.08	-66 24 27.5	13.00	-0.10	B0.7 Ib	307 (12)	Sk-66° 37, P3271; UVES spectrum
N11-016	04 56 20.59	-66 27 14.0	13.05	-0.12	B1 Ib	294 (12)	Sk-66° 26, P1036; UVES spectrum
N11-017	04 56 17.57	-66 18 18.5	13.11	0.02	B0.5 Iab	291 (14)	Sk-66° 23
N11-018	04 56 41.04	-66 24 40.3	13.13*	-0.09	O6 II(f ⁺)	301 (6)	P3053, variable v_r or wind var.?
N11-019	04 56 11.72	-66 31 59.1	13.14	-0.17	O8-9 III-V((f))	Binary (SB2)	Sk-66° 22
N11-020	04 56 50.32	-66 31 03.6	13.18	-0.22	O5 I(n)fp	Binary	H α = broad em.
N11-021	04 56 30.58	-66 18 08.6	13.24	0.12	A7 II	298 (4)	
N11-022	04 56 00.90	-66 26 16.4	13.33	-0.15	O6.5 II(f) var	289 (8)	Sk-66° 20
N11-023†	04 56 15.44	-66 27 34.9	13.40	-0.14	B0.7 Ib	286 (12)	P1014; UVES spectrum
N11-024	04 55 32.93	-66 25 27.7	13.45	-0.10	B1 Ib	292 (12)	
N11-025	04 56 34.84	-66 28 23.1	13.45	0.35	O8.5 V	-	FLAMES-UVES target
N11-026	04 56 52.54	-66 19 55.8	13.51	-0.17	O2.5 III(f [*])	330 (8)	
N11-027	04 56 53.19	-66 19 01.9	13.56	0.68	G2	-	FLAMES-UVES target, foreground
N11-028	04 57 16.24	-66 23 20.8	13.63	0.10	O6-8 V	304 (3)	P3264; strong nebular contamination
N11-029	04 55 56.34	-66 29 03.9	13.63	-0.12	OC9.7 Ib	297 (15)	
N11-030	04 55 48.38	-66 29 41.4	13.66	-0.10	B1e	Binary	H α = broad em.
N11-031	04 56 42.49	-66 25 18.0	13.68*	-0.01	ON2 III (f [*])	322 (6)	P3061
N11-032	04 56 54.46	-66 24 15.6	13.68*	-0.11	O7 II(f)	305 (9)	P3168; no observations in HR02/ λ 3958 region
N11-033	04 56 11.04	-66 28 23.9	13.68	-0.16	B0 III _n	296: (9)	P1005
N11-034	04 56 42.66	-66 29 45.1	13.68	-0.15	B0.5 III	289: (10)	P1332; variable v_r ?
N11-035	04 57 28.70	-66 31 02.4	13.69	0.03	O9 II(f)	Binary (SB1)	
N11-036	04 57 41.00	-66 29 56.4	13.72	-0.15	B0.5 Ib	292 (16)	
N11-037	04 56 22.33	-66 28 04.6	13.77	-0.10	B0 III	Binary (SB1)	P1052
N11-038	04 56 45.21	-66 25 10.6	13.81*	0.00	O5 III(f ⁺)	318 (4)	P3100
N11-039	04 56 17.33	-66 17 48.0	13.83	-0.18	B2 III	286 (9)	
N11-040	04 57 16.72	-66 28 22.7	13.84	-0.10	B0: III _n	Binary?	H α = abs+twin em.
N11-041	04 56 52.32	-66 32 52.5	13.87	-0.19	O6.5 Iaf	Binary	H α = complex abs+broad em.
N11-042	04 56 15.57	-66 27 21.2	13.93	-0.23	B0 III	288 (15)	P1017
N11-043	04 57 01.06	-66 28 29.8	13.93	-0.21	O7 III + B0:	Binary (SB2)	
N11-044	04 57 15.74	-66 33 54.0	13.96	-0.14	O6-8 III-V((f))	Binary (SB2)	early B-type secondary
N11-045	04 56 58.32	-66 31 32.9	13.97	-0.15	O9-9.5 III	290 (13)	
N11-046	04 56 44.62	-66 34 20.5	13.98	-0.24	O9.5 V	Binary	
N11-047	04 56 25.48	-66 26 33.2	14.01	-0.23	B0 III	Binary (SB1)	
N11-048†	04 56 58.79	-66 24 40.7	14.02*	-0.17	O6.5 V((f))	299 (3)	P3204
N11-049	04 56 29.59	-66 28 20.5	14.02	-0.24	O7.5 V	Binary (SB1)	P1110
N11-050	04 57 00.88	-66 23 57.1	14.03	0.10	O4-5 + O7:	Binary (SB2)	P3224
N11-051	04 56 29.72	-66 21 38.5	14.03	-0.26	O5 Vn((f))	296: (5)	
N11-052	04 57 40.12	-66 26 02.8	14.06	-0.18	O9.5 V	Binary (SB2)	
N11-053	04 56 54.48	-66 27 32.0	14.09	-0.16	B1: (Be-Fe)	Binary	
N11-054	04 57 18.33	-66 25 59.6	14.10	-0.06	B1 Ib	294 (12)	
N11-055	04 57 10.57	-66 18 06.8	14.11	0.18	O8-9 III _{ne}	293 (3)	H α = broad em.
N11-056	04 57 49.05	-66 24 17.4	14.13	-0.10	B1e	304 (8)	H α = weak twin em.
N11-057†	04 56 15.48	-66 27 41.5	14.13	0.03	A0 II	284 (4)	P1015
N11-058	04 55 52.35	-66 34 13.4	14.16	-0.23	O5.5 V((f))	301 (3)	
N11-059	04 56 31.02	-66 28 40.8	14.23	-0.25	O9 V	Binary (SB1)	P1125
N11-060	04 56 42.16	-66 24 54.4	14.24*	-0.06	O3 V((f [*]))	314 (3)	P3058
N11-061	04 57 25.73	-66 21 05.4	14.24	-0.06	O9 V	305 (10)	
N11-062	04 56 55.35	-66 33 01.8	14.32	-0.23	B0.2 V	Binary (SB1)	
N11-063	04 57 40.53	-66 27 25.1	14.35	-0.18	O9: Vn	Binary (SB2)	
N11-064	04 57 11.47	-66 22 18.8	14.40	-0.14	B0.2: Vn	Binary	
N11-065	04 56 19.35	-66 27 01.8	14.40	-0.24	O6.5 V((f))	303 (7)	P1027
N11-066	04 56 57.51	-66 35 21.3	14.40	-0.24	O7 V((f))	282 (7)	
N11-067	04 57 03.33	-66 30 08.1	14.50	-0.24	B0.5: Vn	Binary	
N11-068	04 56 04.61	-66 23 57.8	14.55	-0.23	O7 V((f))	291 (10)	
N11-069	04 56 20.80	-66 27 03.3	14.56	-0.19	B1 III	279 (12)	P1037; UVES spectrum
N11-070	04 57 04.61	-66 24 22.3	14.59	-0.13	B3 III	274 (8)	P3239
N11-071	04 57 24.19	-66 26 00.0	14.61	-0.19	O8: V	Binary (SB2)	
N11-072	04 55 51.63	-66 21 57.5	14.61	-0.27	B0.2 V	296 (13)	
N11-073	04 57 11.26	-66 26 53.8	14.63	-0.06	B0.5 (Be-Fe)	288: (6)	H α = broad em.
N11-074	04 56 19.49	-66 27 37.9	14.63	-0.01	B0.5 (Be-Fe)	288: (5)	P1028; H α = broad em.
N11-075	04 57 22.05	-66 19 20.7	14.67	-0.18	B2 III	Binary?	Gaps in spectra due to bad pixels
N11-076	04 56 33.58	-66 23 28.0	14.67	0.33	B0.2 Ia	331 (9)	H α = P Cyg., variable v_r ?
N11-077	04 56 01.36	-66 20 51.2	14.68	-0.14	B2 III	Binary (SB1)	
N11-078	04 56 04.94	-66 31 24.8	14.69	-0.19	B2 (Be-Fe)	Binary (SB1)	H α = broad em.
N11-079	04 56 47.22	-66 24 42.1	14.71*	-0.12	B0.2 V	305 (8)	P3128

continued on next page

Table 6: *continued*

ID	$\alpha(2000)$	$\delta(2000)$	V	$B - V$	Sp. Type	v_r	Comments
N11-080	04 56 54.71	-66 24 54.3	14.71*	-0.15	O7: V + O9:	Binary (SB2)	P3173
N11-081	04 55 17.87	-66 31 49.7	14.72	0.09	B0: n (Be-Fe)	—	H γ = twin em. + str. nebular; <i>HeII</i> λ 4686; $v_r = 286$
N11-082	04 57 32.49	-66 29 49.1	14.72	-0.16	B1-2 +early-B	Binary (SB2)	
N11-083	04 57 00.24	-66 32 16.3	14.73	-0.20	B0.5 V	287 (12)	variable v_r ?
N11-084	04 56 09.20	-66 27 08.5	14.75	-0.21	B0.5 V	306: (8)	
N11-085	04 56 39.34	-66 28 59.0	14.75	-0.16	B0.5 V	293: (10)	variable v_r ?
N11-086	04 56 43.69	-66 28 36.0	14.75	-0.21	B1 V	284 (7)	
N11-087	04 56 39.18	-66 24 50.0	14.76*	-0.10	O9.5 Vn	309 (2)	P3042
N11-088	04 56 32.93	-66 28 52.1	14.78	-0.21	B1 III	281: (6)	P1160
N11-089	04 55 28.33	-66 29 41.6	14.81	-0.03	B2 III	Binary (SB1)	
N11-090	04 57 32.51	-66 25 56.8	14.83	-0.08	B2e	292: (5)	H α = broad em.
N11-091	04 57 01.32	-66 20 13.0	14.85	-0.10	O9 V	Binary	
N11-092†	04 55 54.19	-66 25 01.5	14.87	0.11	O7 V	Binary	
N11-093	04 55 29.95	-66 30 37.5	14.87	-0.14	B2.5 III	293 (10)	
N11-094	04 57 17.08	-66 30 22.5	14.87	-0.18	B1 III	Binary (SB1)	
N11-095	04 57 37.92	-66 24 59.7	14.89	-0.18	B1 Vn	295: (5)	
N11-096	04 56 54.08	-66 21 56.3	14.89	-0.19	B1.5 III	Binary (SB2)	
N11-097	04 55 17.66	-66 27 35.8	14.90	0.05	B3 II	294 (12)	
N11-098	04 56 58.97	-66 34 46.3	14.93	-0.18	B2 III	Binary (SB1)	
N11-099	04 57 46.69	-66 28 27.8	14.93	-0.11	B0.2 V	Binary (SB1)	strong nebular contamination
N11-100	04 57 21.21	-66 25 01.2	14.94	-0.20	B0.5 V	345 (12)	P3270; UVES spectrum
N11-101	04 56 38.12	-66 23 54.2	14.95*	-0.14	B0.2 V	302 (10)	P3033; UVES spectrum
N11-102	04 55 53.84	-66 34 29.4	14.95	-0.16	B0.2 V	296: (5)	
N11-103	04 56 43.96	-66 28 14.5	14.95	-0.14	B1-2 +early-B	Binary	
N11-104	04 55 55.23	-66 21 57.2	14.96	-0.19	B1.5 V	263: (9)	
N11-105	04 56 46.37	-66 27 16.7	14.97*	-0.25	B1 V	295 (8)	P1378; variable v_r ?
N11-106	04 56 42.08	-66 31 19.0	14.99	-0.26	B0 V	290 (13)	
N11-107	04 55 32.90	-66 32 31.3	15.00	-0.14	B1-2 +early-B	Binary (SB2)	
N11-108	04 57 09.31	-66 22 11.8	15.04	-0.18	O9.5 V	306 (15)	
N11-109	04 55 49.10	-66 27 39.1	15.07	0.10	B0.5 Ib	300 (15)	
N11-110	04 57 37.11	-66 23 44.7	15.08	-0.05	B1 III	298 (14)	
N11-111	04 56 05.86	-66 21 54.8	15.11	-0.24	B1.5 III	285 (10)	
N11-112	04 56 58.50	-66 32 43.6	15.12	-0.11	B1 Vn	Binary	
N11-113	04 56 46.72	-66 29 11.4	15.13	-0.26	B0.5 III	Binary (SB2)	Early B-type companion
N11-114	04 57 37.69	-66 24 48.5	15.15	-0.21	B0 Vn	296 (6)	variable v_r ?
N11-115	04 57 43.26	-66 24 38.0	15.15	-0.14	B1 III	299 (10)	
N11-116	04 55 54.80	-66 27 41.8	15.16	-0.07	B2 III	295 (8)	
N11-117	04 57 44.46	-66 23 59.2	15.21	-0.19	B1 Vn	291: (6)	variable v_r ?
N11-118	04 56 44.30	-66 23 04.8	15.21	-0.17	B1.5 V	Binary (SB1)	
N11-119	04 55 49.45	-66 26 03.5	15.22	-0.21	B1.5 V	Binary (SB2)	
N11-120	04 57 15.22	-66 22 29.5	15.24	-0.12	B0.2 Vn	Binary	
N11-121	04 56 44.52	-66 30 03.3	15.24	-0.19	B1 Vn	299: (4)	
N11-122	04 56 28.76	-66 28 47.1	15.27	-0.27	O9.5 V	289 (10)	
N11-123	04 56 50.50	-66 28 23.1	15.29	-0.25	O9.5 V	295 (11)	
N11-124	04 56 18.63	-66 28 37.2	15.34	-0.21	B0.5 V	Binary (SB1)	

†: Further notes on individual stars

N11-023 & N11-057: These two stars are unresolved in the charts of Sanduleak (1969) and together were identified Sk-66°24.

N11-048: Blended with Parker 3209, which together likely comprise Sk-66°33.

N11-092: Blended with another star in the WFI image, which together comprise Sk-66°19.

Table 7: NGC 2004: Observational parameters of target stars. The cross-references in the final column are to Sanduleak (1969, Sk), Robertson (1974, R74), Breysacher (1981, Brey), Walker (1987) and Martayan et al. (2006, MHF). All spectral types are those of the authors, excepting NGC 2004-057 (Brey 45), taken from Smith et al. (1996). Photometry for the first eight stars comes from Ardeberg et al. (1972) and Balona & Jerzykiewicz (1993), as described in the erratum.

ID	$\alpha(2000)$	$\delta(2000)$	r_d	V	$B - V$	Sp. Type	v_r	Comments
NGC 2004-001	05 30 07.07	-67 15 43.3	3.54	11.46	0.05	A1 Ia	314 (6)	Sk-67°143; H α => v_r variable or var. em.
NGC 2004-002	05 31 12.82	-67 15 08.0	3.79	11.60	0.09	A3: Iab	295 (2)	Sk-67°155; FLAMES-UVES target
NGC 2004-003	05 30 40.40	-67 16 09.0	1.09	12.09	-0.06	B5 Ia	309 (12)	R74-C01; binary?
NGC 2004-004	05 31 27.90	-67 24 43.9	8.79	11.95	0.00	B9 Ia	322 (8)	Sk-67°157
NGC 2004-005	05 29 42.61	-67 20 47.5	6.60	11.93	0.04	B8 Ia	313 (10)	Sk-67°137
NGC 2004-006	05 30 01.22	-67 14 36.9	4.59	12.01	0.07	A2 Iab	313 (3)	Sk-67°141
NGC 2004-007	05 32 00.76	-67 20 22.6	8.39	12.04	-0.03	B8 Ia	310 (10)	Sk-67°171
NGC 2004-008	05 30 40.10	-67 16 37.9	0.61	12.43	-0.03	B9 Ia	305 (10)	R74-B01
NGC 2004-009	05 31 52.98	-67 12 15.4	8.61	12.47	0.01	A1 Iab	308 (4)	
NGC 2004-010	05 29 21.72	-67 20 11.0	8.13	12.60	-0.15	B2.5 Iab	296 (12)	Sk-67°133
NGC 2004-011	05 31 03.75	-67 21 20.1	4.69	12.64	-0.13	B1.5 Ia	309 (12)	Sk-67°154
NGC 2004-012	05 30 37.48	-67 16 53.7	0.43	13.39	-0.20	B1.5 Iab	305 (12)	R74-B09
NGC 2004-013	05 30 46.55	-67 19 39.8	2.50	13.40	-0.17	B2 II	289: (10)	R74-D13; H α => v_r variable or var. em.
NGC 2004-014	05 30 44.47	-67 21 01.5	3.81	13.43	-0.12	B3 Ib	306 (12)	
NGC 2004-015	05 29 11.46	-67 15 24.4	8.76	13.48	-0.20	B1.5 II	Binary (SB1)	
NGC 2004-016	05 30 40.11	-67 18 59.1	1.75	13.54	-0.05	B9 Ib	296 (5)	R74-D18
NGC 2004-017	05 30 46.59	-67 14 21.7	2.94	13.55	0.56	G2	-	FLAMES-UVES target; foreground
NGC 2004-018	05 31 02.69	-67 20 49.8	4.20	13.58	0.57	G8:	-	FLAMES-UVES target; foreground
NGC 2004-019	05 30 44.62	-67 18 37.9	1.46	13.60	-0.20	O9.5 III _n	318: (12)	R74-D16
NGC 2004-020	05 30 53.80	-67 15 48.8	1.94	13.61	-0.13	B1.5 II	Binary (SB1)	
NGC 2004-021	05 30 42.01	-67 21 41.4	4.46	13.67	-0.14	B1.5 Ib	311 (12)	
NGC 2004-022	05 30 47.37	-67 17 23.4	0.71	13.77	-0.17	B1.5 Ib	300 (12)	R74-B30
NGC 2004-023	05 30 58.01	-67 18 14.8	1.99	13.91	-0.08	B2 (Be-Fe)	311: (6)	H α = str. em.
NGC 2004-024	05 29 53.99	-67 17 22.2	4.46	14.07	-0.15	B1.5 III _n	356 (7)	
NGC 2004-025	05 30 00.73	-67 21 56.4	6.05	14.17	-0.16	B2 (Be-Fe)	305 (8)	H α = str. em.
NGC 2004-026	05 30 36.35	-67 17 42.9	0.60	14.18	-0.17	B2 II	Binary (SB1)	R74-B15; H α = shell star
NGC 2004-027	05 29 34.53	-67 11 56.1	8.26	14.18	-0.11	B0e	282 (5)	H α & He6678 variable v_r or var. em.?
NGC 2004-028	05 31 32.59	-67 16 40.3	5.09	14.26	-0.19	B2 II	311: (6)	
NGC 2004-029	05 31 00.11	-67 14 59.2	2.96	14.27	-0.20	B1.5e	322 (10)	H α = str. em.
NGC 2004-030	05 30 11.03	-67 22 57.1	6.37	14.28	-0.23	B0.2 Ib	Binary (SB1)	
NGC 2004-031	05 30 38.77	-67 20 23.9	3.16	14.29	-0.16	B2 II	Binary (SB1)	
NGC 2004-032	05 30 37.30	-67 10 34.0	6.68	14.30	-0.14	B2 II	305: (7)	
NGC 2004-033	05 29 32.69	-67 17 05.0	6.52	14.31	-0.18	B1.5e	309 (6)	H α = twin em., var
NGC 2004-034	05 30 28.11	-67 15 16.7	2.28	14.40	-0.11	B1.5e	310 (6)	H α = twin em.
NGC 2004-035	05 30 37.16	-67 15 44.3	1.53	14.40	-0.02	B1: (Be-Fe)	312: (4)	H α = twin em.
NGC 2004-036	05 29 20.73	-67 17 54.8	7.70	14.43	-0.22	B1.5 III	308 (12)	
NGC 2004-037	05 30 26.38	-67 09 00.8	8.33	14.45	-0.10	B2e	270: (4)	H α =twim em, variable v_r ?
NGC 2004-038	05 31 22.14	-67 17 39.1	4.07	14.46	-0.24	B0.7 V	290: (6)	
NGC 2004-039	05 30 27.22	-67 13 27.6	3.98	14.47	-0.11	B1.5e	310: (6)	H α = wk twin em
NGC 2004-040	05 30 07.27	-67 14 23.3	4.27	14.49	0.07	A7 II	292 (3)	
NGC 2004-041	05 30 32.64	-67 15 25.9	1.95	14.52	-0.14	B2.5 III	Binary (SB1)	MHF98013
NGC 2004-042	05 31 11.98	-67 23 14.3	6.74	14.53	-0.18	B2.5 III	294 (10)	
NGC 2004-043	05 30 38.74	-67 15 13.2	2.02	14.58	-0.16	B1.5 III	333 (12)	
NGC 2004-044	05 29 33.98	-67 18 06.9	6.45	14.60	-0.22	B1.5:	Binary (SB2)	Similar temperature secondary; MHF83937
NGC 2004-045	05 30 50.19	-67 14 47.6	2.63	14.60	-0.18	B2 III	Binary (SB1)	
NGC 2004-046	05 30 42.96	-67 16 43.5	0.58	14.64	-0.19	B1.5 III	312 (12)	R74-B50
NGC 2004-047	05 30 13.54	-67 14 27.3	3.79	14.70	-0.21	B2 III	Binary (SB1)	MHF103207
NGC 2004-048	05 31 47.04	-67 17 54.6	6.49	14.70	-0.20	B2.5e	307: (7)	
NGC 2004-049	05 30 06.19	-67 14 32.9	4.24	14.71	-0.24	O2-3 III(f [*]) + OB	Binary (SB2)	
NGC 2004-050	05 30 43.07	-67 17 43.9	0.57	14.71	-0.19	B2.5 III	Binary (SB1)	R74-B24
NGC 2004-051	05 30 53.44	-67 17 10.6	1.28	14.73	-0.19	B2 III	308 (12)	R74-C16
NGC 2004-052	05 32 06.28	-67 19 49.2	8.70	14.75	-0.23	B2 III	291: (10)	
NGC 2004-053	05 30 43.79	-67 15 22.6	1.89	14.75	-0.21	B0.2 Ve	303 (14)	H α = em.
NGC 2004-054	05 31 46.38	-67 13 28.9	7.41	14.76	-0.20	B2 III	Binary (SB1)	
NGC 2004-055	05 30 14.55	-67 15 27.2	3.05	14.76	-0.17	B2.5 III	309: (8)	H α = complex, in-filled from em.
NGC 2004-056	05 30 35.92	-67 11 08.5	6.11	14.84	-0.04	B1.5e	300 (4)	H α = twin em.
NGC 2004-057	05 31 34.37	-67 16 29.4	5.28	14.85	-0.51	WN4b	-	Sk-67°160; Brey 45
NGC 2004-058	05 30 05.13	-67 18 45.8	3.71	14.86	-0.20	O9.5 V (N str)	303: (10)	
NGC 2004-059	05 30 45.92	-67 18 24.4	1.29	14.86	-0.20	B2 III	Binary (SB1)	R74-D17
NGC 2004-060	05 30 32.94	-67 11 22.5	5.91	14.86	-0.14	B2 III	295 (7)	
NGC 2004-061	05 29 15.96	-67 19 45.4	8.51	14.88	-0.25	B2 III	312 (12)	
NGC 2004-062	05 31 10.97	-67 22 51.4	6.36	14.90	-0.23	B0.2 V	319: (8)	
NGC 2004-063	05 30 34.49	-67 17 34.9	0.65	14.93	-0.15	B2 III	311 (8)	R74-C08
NGC 2004-064	05 31 19.11	-67 16 54.7	3.77	14.96	-0.22	B0.7-B1 III	310 (12)	
NGC 2004-065	05 30 13.10	-67 21 06.5	4.67	14.96	-0.19	B2.5 III	306: (7)	
NGC 2004-066	05 30 27.78	-67 17 22.8	1.21	14.96	-0.16	B1.5 Vn	308: (6)	
NGC 2004-067	05 30 34.64	-67 14 45.6	2.54	14.96	-0.08	B1.5e	284: (5)	H α = twin; MHF101350
NGC 2004-068	05 30 23.00	-67 08 53.6	8.51	14.97	-0.08	B2.5 III	281 (10)	
NGC 2004-069	05 30 12.15	-67 10 19.7	7.42	14.99	-0.24	B0.7 V	332 (6)	
NGC 2004-070	05 31 03.61	-67 16 07.7	2.52	15.01	-0.22	B0.7-B1 III	310 (12)	
NGC 2004-071	05 31 31.31	-67 11 33.3	7.53	15.05	-0.23	B1.5 III	298 (9)	
NGC 2004-072	05 29 50.50	-67 15 10.4	5.22	15.08	-0.22	B1.5 V	Binary (SB1)	
NGC 2004-073	05 30 55.73	-67 18 48.6	2.17	15.08	-0.20	B2 III	304 (12)	R74-D12
NGC 2004-074	05 30 29.03	-67 22 52.8	5.74	15.08	-0.19	B0.7-B1 V	Binary (SB1)	
NGC 2004-075	05 30 53.42	-67 18 03.7	1.52	15.08	-0.18	B2 III	289: (11)	R74-D10
NGC 2004-076	05 30 20.65	-67 08 41.2	8.76	15.08	-0.08	B2.5 III	Binary (SB1)	
NGC 2004-077	05 29 16.94	-67 20 33.8	8.70	15.09	-0.29	B0.5 V	296: (6)	
NGC 2004-078	05 31 31.33	-67 15 05.9	5.38	15.09	-0.20	B2 III	Binary (SB1)	

continued on next page

Table 7: *continued*

ID	$\alpha(2000)$	$\delta(2000)$	r_d	V	$B - V$	Sp. Type	v_r	Comments
NGC 2004-079	05 30 40.75	-67 11 43.9	5.51	15.09	-0.16	B2 III	Binary (SB1)	
NGC 2004-080	05 29 58.83	-67 16 17.8	4.10	15.11	-0.21	B2.5 III	313 (10)	
NGC 2004-081	05 29 52.86	-67 18 14.6	4.68	15.11	-0.20	B1 V	298 (8)	
NGC 2004-082	05 30 20.37	-67 20 55.4	4.15	15.11	-0.19	B1.5 V	305: (7)	
NGC 2004-083	05 30 28.43	-67 17 00.6	1.16	15.11	-0.11	B1.5: e	Binary (SB1)	R74-D22; H α = twin
NGC 2004-084	05 31 08.01	-67 20 00.3	3.85	15.14	-0.21	B1.5 III	306 (12)	
NGC 2004-085	05 29 56.32	-67 17 55.5	4.29	15.14	-0.19	B2.5 III	305: (10)	
NGC 2004-086	05 30 58.02	-67 14 04.8	3.60	15.15	-0.20	B2 III	312 (10)	
NGC 2004-087	05 31 01.27	-67 20 08.7	3.55	15.15	-0.20	B1.5 V	316 (12)	
NGC 2004-088	05 30 57.15	-67 15 14.3	2.58	15.15	-0.18	B2.5 III	307: (5)	No λ 4124 data
NGC 2004-089	05 30 48.35	-67 21 58.6	4.80	15.16	-0.14	B2.5e	304: (9)	H α = twin
NGC 2004-090	05 29 22.31	-67 16 40.1	7.54	15.17	-0.28	O9.5 III	310 (16)	
NGC 2004-091	05 29 34.32	-67 15 01.9	6.73	15.17	-0.22	B1.5 III	310 (12)	
NGC 2004-092	05 30 24.95	-67 12 46.8	4.70	15.18	-0.11	B2e	304: (5)	H α = twin
NGC 2004-093	05 29 20.33	-67 19 04.3	7.92	15.19	-0.21	B3 III	287: (9)	
NGC 2004-094	05 31 09.27	-67 15 22.3	3.37	15.20	-0.19	B2.5 III	Binary	
NGC 2004-095	05 30 59.22	-67 15 31.7	2.51	15.20	-0.19	B1.5 V	287 (8)	
NGC 2004-096	05 30 29.95	-67 15 53.5	1.67	15.21	-0.09	B1.5e	317: (4)	H α = twin
NGC 2004-097	05 30 13.21	-67 08 40.4	8.95	15.24	-0.20	B2 III	298 (10)	variable v_r ?
NGC 2004-098	05 31 00.30	-67 19 05.9	2.69	15.24	-0.18	B2 III	287: (7)	
NGC 2004-099	05 31 16.52	-67 20 55.7	5.09	15.26	-0.21	B2 III	292: (7)	
NGC 2004-100	05 29 29.89	-67 18 22.1	6.88	15.29	-0.18	B1 Vn	298: (6)	
NGC 2004-101	05 30 48.23	-67 17 13.0	0.78	15.30	-0.18	B2 III	309: (10)	R74-B28
NGC 2004-102	05 31 00.23	-67 16 04.0	2.26	15.30	-0.18	B2 III	Binary	
NGC 2004-103	05 30 20.63	-67 13 40.7	4.03	15.30	-0.12	B2 III	303 (11)	
NGC 2004-104	05 29 38.76	-67 12 07.6	7.83	15.31	-0.19	B1.5 V	301: (6)	
NGC 2004-105	05 30 10.20	-67 18 42.3	3.25	15.31	-0.19	B1.5 V	297: (7)	
NGC 2004-106	05 30 29.49	-67 16 46.0	1.14	15.31	-0.14	B2 III	307 (11)	R74-D23; Walker 4
NGC 2004-107	05 31 45.13	-67 23 01.8	8.53	15.32	-0.25	B0.5 V	Binary (SB1)	
NGC 2004-108	05 30 18.15	-67 12 58.6	4.76	15.32	-0.21	B2.5 III	296 (10)	
NGC 2004-109	05 29 11.05	-67 18 59.2	8.78	15.32	-0.20	B2.5 III	298: (11)	MHF79301
NGC 2004-110	05 30 50.48	-67 10 38.4	6.67	15.32	-0.19	B2 III	296: (7)	
NGC 2004-111	05 32 05.74	-67 15 58.1	8.35	15.39	-0.21	B2.5 III	310 (10)	
NGC 2004-112	05 32 04.73	-67 19 03.7	8.36	15.39	-0.19	B2 III	307 (8)	
NGC 2004-113	05 30 53.86	-67 16 54.4	1.36	15.39	-0.17	B2.5 III _n	293: (7)	R74-D08
NGC 2004-114	05 30 47.87	-67 24 45.4	7.55	15.43	-0.18	B2 III	298 (11)	
NGC 2004-115	05 31 04.64	-67 18 35.1	2.72	15.44	-0.19	B2e	Binary (SB1)	H α = twin+central abs
NGC 2004-116	05 30 23.58	-67 10 41.7	6.74	15.44	-0.12	B2 III	309 (13)	H α => v_r variable or var. em.
NGC 2004-117	05 30 29.14	-67 09 51.2	7.46	15.47	-0.14	B2 III	305 (10)	
NGC 2004-118	05 31 17.28	-67 18 42.5	3.87	15.52	-0.21	B1.5 V	Binary (SB1)	
NGC 2004-119	05 31 14.65	-67 11 59.8	6.21	15.53	-0.20	B2 III	309 (14)	

Table 8: Comparison of current classifications with published spectral types. Sources of classifications are W77 (Walborn 1977); FB80 (Feast & Black 1980); CJF85 (Carney et al. 1985); NMC (Niemela et al. 1986); G87 (Garmany et al. 1987); MPG (Massey et al. 1989); F91 (Fitzpatrick 1991); P92 (Parker et al. 1992); L93 (Lennon et al. 1993); M95 (Massey et al. 1995); G96 (Grebel et al. 1996); LG96 (classifications from Lennon, given by Grebel et al. 1996); HM00 (Heydari-Malayeri et al. 2000, who adopt identifications from Woolley 1963); W00 (Walborn et al. 2000); L03 (Lennon et al. 2003); EH04 (Evans et al. 2004).

ID	Alias	FLAMES	Published
NGC 346-001	AzV 232/Sk 80	O7 Iaf+	O7 Iaf+ [W77]; O7 If [MPG 789]
NGC 346-004	AzV 191	Be (B1:)	B extr [G87]
NGC 346-007	MPG 324	O4 V((f+))	O4-5 V [NMC]; O4 V((f)) [MPG]; O4 ((f)) [W00]
NGC 346-008	AzV 224	B1e	B1 III [G87]
NGC 346-009	MPG 845	B0e	O9.5 V [MPG]
NGC 346-010	AzV 226	O7 IIIIn((f))	O7 III [G87]
NGC 346-012	AzV 202	B1 Ib	B1 III [G87]
NGC 346-014	2dFS#1425	A0 II	A0 (Ib) [EH04]
NGC 346-015	AzV 217	B1 V +?	B1 III [M95]; B1-3 (II) [EH04: 2dFS#1357]
NGC 346-016	2dFS#5100	B0.5 Vn +?	B0-3 (III) [EH04]
NGC 346-020	2dFS#1259	B1 V+early-B	B0-3 (III) [EH04]
NGC 346-021	2dFS#5099	B1 III	B1-3 (III) [EH04]
NGC 346-022	MPG 682	O9 V	O8 V [MPG]
NGC 346-023	MPG 178	Be (B0.2:)	O8-8.5 V:: [MPG]; B0: (IV) [EH04: 2dFS#5097]
NGC 346-025	MPG 848	O9 V	O8.5 V [MPG]
NGC 346-026	MPG 12	B0 IV (Nstr)	O9.5 V [MPG]; O9.5-B0 V (N str) [W00]; O9.5 III [EH04: 2dFS#1299]
NGC 346-028	MPG 113	OC6 Vz	O6 V [MPG]; OC6 Vz [W00, the source of the type adopted here]
NGC 346-029	MPG 637	B0 V +?	B0 V [MPG]
NGC 346-030	2dFS#5098	B0 V +?	B0.5 (V) [EH04]
NGC 346-034	MPG 467	O8.5 V	O8 V+neb [MPG]
NGC 346-035	2dFS#1418	B1 V +?	B1-5 (II) [EH04]
NGC 346-036	MPG 729	B0.5 Ve	B0+neb [MPG]
NGC 346-039	2dFS#1262	B0.7 V	B1-3 (III) [EH04]
NGC 346-043	MPG 11	B0 V	B0 V [MPG]
NGC 346-047	2dFS#1189	B2.5 III	B1-5 (III) [EH04]
NGC 346-050	MPG 299	O8 Vn	O9 V [MPG]
NGC 346-051	MPG 523	O7 Vz	O7 V+neb [MPG]
NGC 346-056	MPG 310	B0 V	O9.5 V [MPG]
NGC 346-061	2dFS#1277	Be (B1-2)	B1-5 (II)e [EH04]
NGC 346-063	2dFS#1413	A0 II	A0 (II) [EH04]
NGC 346-075	2dFS#1389	B1 V +?	B1-3 (IV) [EH04]
NGC 346-077	MPG 238	O9 V	B0: [MPG]
NGC 346-084	2dFS#1296	B1 V	B0-5 (IV) [EH04]
NGC 330-002	R74-A02	B3 Ib	B5 I [FB80]; B6 I [CJF85]; B4 Iab/b [L93]; B5 I [G96]; B4 Ib [L03]
NGC 330-003	2dFS#1183	B2 Ib	B2.5 (Ib) [EH04]
NGC 330-004	R74-B37	B2.5 Ib	B5 I [FB80]; B5 I [CJF85]; B3 Ib [L93]; B2.5 (Ib) [EH04: 2dFS#5090]
NGC 330-012	Arp 211	A0 Ib	A0 I [CJF85]
NGC 330-013	AzV 186	O8 III ((f))	O7 III [G87]; O8 III((f)) [EH04: 2dFS#1230]
NGC 330-017	2dFS#1171	B2 II	B1-3 (II) [EH04]
NGC 330-018	R74-B30	B3 II	B6 I [CJF85]; B2 II [L93]
NGC 330-020	2dFS#1232	B3 II	B3 (II) [EH04]
NGC 330-021	2dFS#1242	B0.2 III	B0.5 (IV) [EH04]
NGC 330-022	2dFS#1062	B3 II	B3 (II) [EH04]
NGC 330-024	2dFS#1034	B5 Ib	B5 (II) [EH04]
NGC 330-025	2dFS#1224	B1.5e	B2 (II) [EH04]
NGC 330-028	2dFS#1195	B1 V	B2 (III) [EH04]
NGC 330-029	2dFS#5093	B0.2 Ve	B0-3 (III)e [EH04]
NGC 330-031	2dFS#5088	B0.5 Ve	B0.5 (IV) [EH04]
NGC 330-033	2dFS#5094	B1.5 V	B1-5 (II) [EH04]
NGC 330-036	R74-B32	B2 II	B2 III [L03]
NGC 330-037	2dFS#1058	A2 II	A0 (II) [EH04]

continued on next page

Table 8: *continued*

ID	Alias	FLAMES	Published
NGC 330-038	2dFS#1206	B1 V	B1-2 (III) [EH04]
NGC 330-039	2dFS#1109	B0 V	B0.5 (V) [EH04]
NGC 330-040	2dFS#1041	B2 III	B1-2 (III) [EH04]
NGC 330-041	2dFS#1241	B0 V	B0 (V) [EH04]
NGC 330-045	2dFS#5087	B3 III	B1-5 (III) [EH04]
NGC 330-046	2dFS#1293	O9.5 V	B0 (V) [EH04]
NGC 330-047	2dFS#1190	B1 V	B1-3 (III) [EH04]
NGC 330-051	2dFS#1276	B1.5 V	B1-5 (III) [EH04]
NGC 330-052	2dFS#1152	O8.5 Vn	O8 V [EH04]
NGC 330-061	2dFS#1118	A0 II	A0 (II) [EH04]
NGC 330-073	2dFS#1087	B8 Ib	B8 (II) [EH04]
NGC 330-104	2dFS#1037	B0: V	B0-5 (IV) [EH04]
NGC 330-118	2dFS#1013	B1-2	B1-2 (V) [EH04]
NGC 330-121	R74-B38	A5 II	A1 I [FB80]
NGC 330-123	R74-B18	O9.5 V	B0 Ve [L93]; O9 III/Ve [LG96]
NGC 330-124	R74-B28	B0.2 V	B0 Ve [L93]; B0.2 IIIe [LG96]
NGC 330-125	R74-B13	B2 III	B2 III/IVe [L93]; B2 III/IVe [LG96]
N11-001	Sk-66°36/P3252	B2 Ia	B2 I + neb [F91]; B2 II (Hwk) [P92]
N11-002	Sk-66°27/P1062	B3 Ia	B2.5-3 Ia [F91]; B4 Ia [P92]
N11-003	P3157	B1 Ia	BC1 Ia (Nwk) [P92]
N11-010	P1310	O9.5 III + B1-2:	B0 V [P92]
N11-013	P3223	O8 V	O8.5 IV [P92]
N11-015	Sk-66°37/P3271	B0.7 Ib	B1 II (Hwk) [P92]
N11-016	Sk-66°26/P1036	B1 Ib	B1.5 Ia (Nwk) [P92]; B1 III [M95]
N11-018	P3053	O6 II(f*)	O5.5 I-III(f) [P92]
N11-022	Sk-66°20	O6.5 II(f)	O6 III [M95]
N11-023	P1014	B0.7 Ib	B0.5 II (blend?) [P92]
N11-028	P3264	O6-8 V	O3-6 V (ZAMS in N11A) [P92]
N11-031	P3061	ON2 III(f*)	O3 III(f*) [P92]; O2 III(f*) [W02]; ON2 III(f*) [W04, adopted here]
N11-032	P3168	O7 II(f)	O7 II(f) [P92]
N11-033	P1005	B0 III _n	B0 III [P92]
N11-034	P1332	B0.5 III	B0.7 II [P92]
N11-037	P1052	B0 III	B0.2 III [P92]
N11-038	P3100	O5 II(f+)	O6.5 V((f)): [P92]
N11-042	P1017	B0 III	B0 III [P92]
N11-048	P3204	O6.5 V((f))	O6-7 V (ZAMS) [P92]
N11-049	P1110	O7.5 V	O7.5 V [P92]
N11-050	P3224	O4-5 + O7:	O6 III (blend?) [P92]
N11-059	P1125	O9 V	O8.5 V [P92]
N11-060	P3058	O3 V((f*))	O3 V((f*)) [P92]; O3 V((f*)) [W02, adopted here]
N11-063	Wo597	O9: V _n	O9 V [HM00]
N11-065	P1027	O6.5 V((f))	O6.5 V((f)) [P92]
N11-069	P1037	B1 III	B1.5 II [P92]
N11-070	P3239	B3 III	B2 V [P92]
N11-074	P1028	B0.5e	O8-9: III: [P92]
N11-079	P3128	B0.2 V	O9.5 IV [P92]
N11-080	P3173	O7: V + O9:	O4-6 V [P92]
N11-087	P3042	O9.5 V _n	O9.5: III: [P92]
N11-088	P1160	B1 III	B1 V [P92]
N11-099	Wo622	B0.2 V	O9.7 III/B0.2 V [HM00]
N11-100	P3270	B0.5 V	B1 V [P92]
N11-101	P3033	B0.2 V	B0.2 IV [P92]
N11-105	P1378	B1 V	B1 V [P92]
NGC 2004-001	Sk-67°143	A1 Ia	B7 Ia+ [F91]

Fig. 13. FLAMES targets in the NGC 346 field. Due to crowding in the core of the cluster 346-007, 034, 079, 086, 111, and 115 are not labelled. Each of these is included in the Massey et al. (1989) study and the reader is referred to their finding charts for these stars.

Fig. 14. FLAMES targets in the NGC 330 field. The five additional UVES targets (nos. 121-125) are not included, the reader is directed to the finding charts by Robertson (1974).

Fig. 15. FLAMES targets in the N11 field. The nine additional UVES targets are not included, the reader is directed to the finding charts by Parker et al. (1992).

Fig. 16. FLAMES targets in the NGC 2004 field.

Fig. 17. O-type (open blue circles) and B-type (gold) FLAMES & UVES targets in the N11 field

Appendix A: Detailed record of observations

Following the detailed discussion of numerous binaries in this paper, for completeness we also include the Modified Julian Dates (MJD) of each of our observations in Tables A.1, A.2, A.3, and A.4.

Table A.1. Modified Julian Dates (MJD) of the NGC 346 FLAMES observations. The Giraffe wavelength settings (e.g. HR02) and central wavelengths (λ_c) are given. The exposure time for each observation was 2275s, excepting HR06/#08, for which it was 2500s.

Giraffe setting	λ_c	#	MJD
HR02	3958	01	52954.135894
HR02	3958	02	52954.162910
HR02	3958	03	52954.189858
HR02	3958	04	52955.089567
HR02	3958	05	52955.116573
HR02	3958	06	52955.143518
HR03	4124	01	52981.045452
HR03	4124	02	52981.072478
HR03	4124	03	52981.099430
HR03	4124	04	52981.132751
HR03	4124	05	52981.159698
HR03	4124	06	52981.186653
HR04	4297	01	52989.130391
HR04	4297	02	52989.157348
HR04	4297	03	52989.184302
HR04	4297	04	53005.048810
HR04	4297	05	53005.075776
HR04	4297	06	53005.102733
HR05	4471	01	52978.115490
HR05	4471	02	52978.142443
HR05	4471	03	52978.169401
HR05	4471	04	53006.047328
HR05	4471	05	53006.074344
HR05	4471	06	53006.101307
HR06	4656	01	52926.086233
HR06	4656	02	52926.138196
HR06	4656	03	52926.165224
HR06	4656	04	52926.203441
HR06	4656	05	52926.230394
HR06	4656	06	52988.111039
HR06	4656	07	52988.155055
HR06	4656	08	52988.183316
HR14	6515	01	52922.133208
HR14	6515	02	52922.177677
HR14	6515	03	52922.204633
HR14	6515	04	52922.240118
HR14	6515	05	52922.267069
HR14	6515	06	52922.308471
HR14	6515	07	52925.152684
HR14	6515	08	52925.179646
HR14	6515	09	52925.206601

Table A.2. Modified Julian Dates (MJD) of the NGC 330 FLAMES observations. The Giraffe wavelength settings (e.g. HR02) and central wavelengths (λ_c) are given. The exposure time for each observation was 2275s, excepting HR02/#06 (1743s); HR05/#05 (2221s); HR04/#06 (1900s).

Giraffe setting	λ_c	#	MJD
HR02	3958	01	52831.335190
HR02	3958	02	52831.362917
HR02	3958	03	52831.389880
HR02	3958	04	52833.343405
HR02	3958	05	52833.380020
HR02	3958	06	52833.407722
HR02	3958	07	52834.272660
HR02	3958	08	52834.310219
HR02	3958	09	52834.338165
HR03	4124	01	52832.306332
HR03	4124	02	52832.334079
HR03	4124	03	52832.361042
HR03	4124	04	52832.389991
HR03	4124	05	52832.417687
HR03	4124	06	52833.431610
HR03	4124	07	53571.338966
HR03	4124	08	53571.365957
HR03	4124	09	53571.392904
HR03	4124	10	53575.350926
HR03	4124	11	53575.377924
HR03	4124	12	53575.404861
HR04	4297	01	52835.365846
HR04	4297	02	52835.392841
HR04	4297	03	52835.419862
HR04	4297	04	52839.383749
HR04	4297	05	52839.410778
HR04	4297	06	52839.435562
HR05	4471	01	52836.311151
HR05	4471	02	52836.338693
HR05	4471	03	52836.365649
HR05	4471	04	52836.406499
HR05	4471	05	52836.433197
HR05	4471	06	52837.228526
HR05	4471	07	52837.255493
HR05	4471	08	52837.282458
HR05	4471	09	52837.409609
HR05	4471	10	52839.296100
HR05	4471	11	52839.323059
HR05	4471	12	52839.350034
HR06	4656	01	52834.365133
HR06	4656	02	52834.400818
HR06	4656	03	52834.428742
HR06	4656	04	52837.320664
HR06	4656	05	52837.347739
HR06	4656	06	52837.375036
HR14	6515	01	52829.311413
HR14	6515	02	52829.339117
HR14	6515	03	52829.366074
HR14	6515	04	52830.302236
HR14	6515	05	52830.329997
HR14	6515	06	52830.356985

Table A.3. Modified Julian Dates (MJD) of the N11 FLAMES observations. The Giraffe wavelength settings (e.g. HR02) and central wavelengths (λ_c) are given. The exposure time for each observation was 2275s.

Giraffe setting	λ_c	#	MJD
HR02	3958	01	52928.313905
HR02	3958	02	52928.340935
HR02	3958	03	52928.367887
HR02	3958	04	52978.209107
HR02	3958	05	52978.236069
HR02	3958	06	52978.263031
HR03	4124	01	52978.298954
HR03	4124	02	52978.325913
HR03	4124	03	52978.352876
HR03	4124	04	52979.120168
HR03	4124	05	52979.147117
HR03	4124	06	52979.174080
HR04	4297	01	52979.209306
HR04	4297	02	52979.236270
HR04	4297	03	52979.263219
HR04	4297	04	52979.297524
HR04	4297	05	52979.324479
HR04	4297	06	52979.351427
HR05	4471	01	52980.104396
HR05	4471	02	52980.131349
HR05	4471	03	52980.158315
HR05	4471	04	52980.193917
HR05	4471	05	52980.220880
HR05	4471	06	52980.247825
HR06	4656	01	52980.282525
HR06	4656	02	52980.309565
HR06	4656	03	52980.336517
HR06	4656	04	52981.222102
HR06	4656	05	52981.249059
HR06	4656	06	52981.276019
HR14	6515	01	52924.309781
HR14	6515	02	52924.336804
HR14	6515	03	52924.363751
HR14	6515	04	52955.178138
HR14	6515	05	52955.205160
HR14	6515	06	52955.232125

Table A.4. Modified Julian Dates (MJD) of the NGC 2004 FLAMES observations. The Giraffe wavelength settings (e.g. HR02) and central wavelengths (λ_c) are given. The exposure time for each observation was 2275s, excepting HR06/#06 (1468s).

Giraffe setting	λ_c	#	MJD
HR02	3958	01	52982.201147
HR02	3958	02	52982.228098
HR02	3958	03	52982.255044
HR02	3958	04	52988.219081
HR02	3958	05	52988.250594
HR02	3958	06	52988.277546
HR03	4124	01	53005.136738
HR03	4124	02	53005.163753
HR03	4124	03	53005.190706
HR03	4124	04	53005.221334
HR03	4124	05	53005.248354
HR03	4124	06	53005.275313
HR04	4297	01	53006.135301
HR04	4297	02	53006.162257
HR04	4297	03	53006.189220
HR04	4297	04	53008.047982
HR04	4297	05	53008.075016
HR04	4297	06	53008.101980
HR05	4471	01	53008.163059
HR05	4471	02	53008.190005
HR05	4471	03	53008.216952
HR05	4471	04	53009.161824
HR05	4471	05	53009.188777
HR05	4471	06	53009.215739
HR06	4656	01	53012.095573
HR06	4656	02	53012.122595
HR06	4656	03	53012.149545
HR06	4656	04	53012.183447
HR06	4656	05	53012.210458
HR06	4656	06	53012.232744
HR14	6515	01	52955.266266
HR14	6515	02	52955.293277
HR14	6515	03	52955.320221
HR14	6515	04	52989.259276
HR14	6515	05	52989.286232
HR14	6515	06	52989.313190

Erratum

Incorrect photometry was given for a total of ten bright stars in Tables 6 and 7. These targets were saturated in the Wide Field Imager (WFI) frames and should have been replaced with published values as given below in Table A.5. Values for the two stars in N11 are taken from Parker et al. (1992). NGC 2004-003 and NGC 2004-008 are from Balona & Jerzykiewicz (1993), with the remaining six from Ardeberg et al. (1972). The only consequence of these changes for the published version is the position of these stars in the Hertzsprung-Russell diagrams in Figure 12. These were used for a qualitative discussion of the populations in each FLAMES field – because of the difference in reddenings the two apparently massive stars in N11 (with $\log(T_{\text{eff}}) \sim 4.2$ and 4.3) will have lower luminosities, therefore corresponding to lower-mass evolutionary tracks.

Table A.5. Replacement photometry for bright stars in Tables 6 and 7 of the published version. These values have been corrected in Tables 6 and 7 of the replacement astro-ph copy.

ID	α (2000)	δ (2000)	V	$B - V$
N11-001	04 57 08.85	−66 23 25.1	11.35	0.06
N11-002	04 56 23.51	−66 29 51.7	11.90	0.37
NGC 2004-001	05 30 07.07	−67 15 43.3	11.46	0.05
NGC 2004-002	05 31 12.82	−67 15 08.0	11.60	0.09
NGC 2004-003	05 30 40.40	−67 16 09.0	12.09	−0.06
NGC 2004-004	05 31 27.90	−67 24 43.9	11.95	0.00
NGC 2004-005	05 29 42.61	−67 20 47.5	11.93	0.04
NGC 2004-006	05 30 01.22	−67 14 36.9	12.01	0.07
NGC 2004-007	05 32 00.76	−67 20 22.6	12.04	−0.03
NGC 2004-008	05 30 40.10	−67 16 37.9	12.43	−0.03

We have also noticed two typographical errors in the published version. The classification for N11-020 should be given in Sections 5.5 and 8.2, and Table 6 as O5 I(n)fp. Secondly, in the heading of Table 7, the number in the parentheses after α should, of course, read ‘(2000)’.

This figure "4988fig13.jpg" is available in "jpg" format from:

<http://arxiv.org/ps/astro-ph/0606405v2>

This figure "4988fig14.jpg" is available in "jpg" format from:

<http://arxiv.org/ps/astro-ph/0606405v2>

This figure "4988fig15.jpg" is available in "jpg" format from:

<http://arxiv.org/ps/astro-ph/0606405v2>

This figure "4988fig16.jpg" is available in "jpg" format from:

<http://arxiv.org/ps/astro-ph/0606405v2>

This figure "4988fig17.jpg" is available in "jpg" format from:

<http://arxiv.org/ps/astro-ph/0606405v2>